

# Evanescent Wave Spectroscopy using Hollow Cylindrical Waveguide Probes

By  
Deirdre Coleman

A Thesis presented to  
Dublin City University

For the degree of Master of Science

June 1996

Supervisor Dr Vincent Ruddy  
School of Physical Sciences  
Dublin City University  
Ireland

### Declaration

I hereby certify that this material, which I now submit for assessment on the programme of study leading to the award of Master of Science is entirely my own work and has not been taken from the work of others save to and to the extent that such work has been cited and acknowledged within the text of my work

Signed Deirdre Colman

ID Number 94970840

Date 8 - July - 1996

**Dedication**

For Mam and Dad

## Acknowledgements

I would like to thank Dr Vince Ruddy for his unending help and guidance throughout this project. I would also like to show my appreciation to my fellow members in the Optical Sensors Group, both old and new, for their companionship and brain power. Vincent Murphy, Tom Butler, Ger O'Keeffe, James Walsh, Fergus Connolly.

Thanks are due also to Des Lavelle for his creative skills, Joe Maxwell and Al Devine for help and advice in crisis management.

Finally, thanks to Damien especially, and all my friends in the Physics Department.

## Abstract

Optical waveguides carry bound modes which consist of a core E and H field, which is oscillatory across the waveguide and evanescent in the waveguide cladding. Both the core and cladding component of each mode has the same frequency and propagation constant. When the frequency of the light carried by the waveguide matches an absorption transition of the material of the cladding, the mode loses optical power as it propagates due to the attenuation of the evanescent cladding portion of the mode. This process is called attenuated total reflection spectroscopy (ATR) or evanescent wave spectrophotometry. As in simple transmission spectrophotometry the absorbance of the mode is related to the interaction length of the waveguide with the absorbing cladding, the concentration of the absorbing species of the cladding and the fraction of the optical power in the evanescent waves of the various modes.

This work firstly represents a theoretical analysis of the bound modes that can exist in a step index hollow cylindrical waveguide, their evanescent power fraction and the effective length of such a waveguide when located in an absorbing cladding material. The waveguide is found to have a normalized frequency or effective V number whose magnitude determines the total number of bound modes and influences the mean evanescent power fraction between modes. This effective V number reduces to that of the solid step index fiber waveguide in the limit of a zero radius inner cavity. Likewise the expression for the mean evanescent mode power fraction becomes - in the limit of zero inner radius - identical to that of the fiber waveguide. The evanescent absorbance of such a hollow waveguide located in an absorbing fluid is modeled in terms of the bulk absorption coefficient of the fluid and the waveguide dimensions.

In the second part of the thesis a set of experimental absorbance values for ATR spectrophotometry using a hollow silica waveguide probe are reported. Good correspondence is found between the theoretical model and the experimental data.

*Schematic of Hollow Waveguide Evanescent Probe*

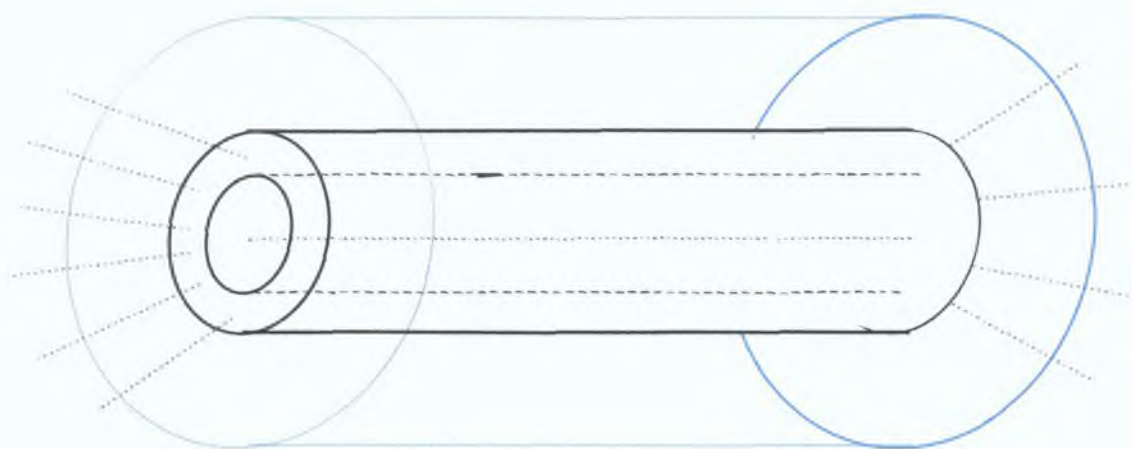


## *Table of Contents*

<b>1 INTRODUCTION TO EVANESCENT WAVE SPECTROPHOTOMETRY</b>	<b>1</b>
1.1 Modes in Waveguides	1
1.2 The Planar Waveguide	3
1.3 The Cylindrical Waveguide.	4
1.4 The Evanescent Power Fraction	7
1.5 The Waveguide as a Sensor	8
1.6 Absorbance of a Sensor Probe	9
1.7 Conclusions	10
1.8 References	11
<b>2 THE HOLLOW CYLINDRICAL WAVEGUIDE - A THEORETICAL MODE ANALYSIS</b>	<b>12</b>
2.1 Introduction	12
2.2 The E and H fields of modes in a hollow waveguide	12
2.3 The mode eigenvalue equation	15
2.4 Mode cut-off condition	18
2.5 Mode indices ( $l, m$ )	20
2.6 Limiting values of $l$ and $m$	22
2.7 The total number of bound modes	22
2.8 An effective V number for the waveguide ( $V'$ )	23
2.9 The mode power in core and cladding	23
2.10 The evanescent power fraction of a mode	24
2.11 Conclusions	24
2.12 References	25
<b>3 MODEL OF HOLLOW CYLINDRICAL WAVEGUIDES - A COMPUTATIONAL ANALYSIS</b>	<b>26</b>
3.1 Introduction	26
3.2 Program to determine mode cut-off values	26

3 3 Computer program to solve the eigenvalue equation	29
3 4 Program to derive E and H field component amplitudes in core and cladding	29
3 5 Program to evaluate mean evanescent power fraction $\bar{f}$ among modes	30
3 6 Mode power fraction distribution	33
3 7 Dependence of $f$ on $V'$ and $(b/a)$	35
3 8 Dependence of $N$ on $V'$	37
3 9 Conclusions	39
3 9 References	40
<b>4 EVANESCENT WAVE SPECTROPHOTOMETRY USING A HOLLOW WAVEGUIDE PROBE</b>	<b>41</b>
4 1 Introduction	41
4 2 The ATR probe	41
4.3 Excitation of modes in the probe	41
4 4 Theoretical absorbance of hollow waveguide probe	43
4.5 Absorbance measurement technique	45
4 6 Conclusions	47
<b>5 EXPERIMENTAL ABSORBANCES USING HOLLOW SILICA WAVEGUIDE</b>	<b>48</b>
5 1 Introduction	48
5 2 Bulk properties of the absorbing cladding	48
5.3 Evanescent absorbance as a function of probe immersion depth	49
5 4 The experimental $\bar{f}$ value	51
5 5 Conclusions	52
5 6 References	53
<b>APPENDIX A CUTS M</b>	<b>A-1</b>
<b>APPENDIX B CUTOUT M</b>	<b>B-1</b>
<b>APPENDIX C HOLL M</b>	<b>C-1</b>
<b>APPENDIX D HOLL_SE M</b>	<b>D-1</b>



<b>APPENDIX E HOLLPOW M</b>	<b>E-1</b>
<b>APPENDIX F MODES M</b>	<b>F-1</b>
<b>APPENDIX G REFLECTION COEFFICIENT</b>	<b>G-1</b>
<b>APPENDIX H 6X6 MATRIX</b>	<b>H-1</b>

## TABLE OF FIGURES

Figure 1-1 The propagation constant $\beta$ of a particular mode	1
Figure 1-2 A Planar Waveguide	3
Figure 1-3 Cylindrical Waveguide	4
Figure 1-4 Power distribution in a waveguide	9
Figure 2-1 Hollow cylindrical waveguide	12
Figure 2-2 Radial E field of (3, 3) mode	17
Figure 2-3 Radial E field in three dimensions	18
Figure 2-4 Example of $l$ versus $m$ graph	21
Figure 3-1 Flow-chart of program Cuts $m$	27
Figure 3-2 Flow-chart of Holl $m$	28
Figure 3-3 Flow-chart for Holl $se\ m$	31
Figure 3-4 Flow-chart for Holl $pow\ m$ (continued in figure 3-5)	32
Figure 3-5 Continuation of flow-chart for Holl $pow\ m$	33
Figure 3-6 Histogram of power fraction $f$ distribution	34
Figure 3-7 $f$ versus $1/V'$ , $C = 1.5$	35
Figure 3-8 $f$ versus $1/V'$ , $C = 1.2$	36
Figure 3-9 Graph of $\bar{f}$ versus $C$	37
Figure 3-10 $C = 1.5$	38
Figure 3-11 $C = 1.2$	38
Figure 4-1 Aluminum plug with fibers attached	42
Figure 4-2 Light being focused into fiber bundle	43
Figure 4-3 Example of saturation of absorbance with increasing depth	45
Figure 5-1 Bulk absorbance versus solution concentration	49
Figure 5-2 Evanescent absorbance versus depth (28.756 $\mu M$ solution)	50
Figure 5-3 Evanescent absorbance versus depth, (306.902 $\mu M$ concentration)	51
Figure G-1 Reflection and transmission at an interface between two media	G-1
Figure G-2 Light ray undergoing total internal reflection	G-2
Table 3-1 $f$ values with corresponding mode percentages	34

# 1. Introduction to evanescent wave spectrophotometry.

## 1.1 Modes in Waveguides.

When light travels within a waveguide, the path that the light follows is defined by the shape and dimensions of the waveguide. According to wave theory, the electromagnetic E and H fields must also be solutions of the wave equation

$$\nabla^2 E - \frac{1}{v_p^2} \frac{\partial^2 E}{\partial t^2} = 0 \quad v_p = \frac{c}{n} \quad \text{Eqn 1.1.1}$$

These allowed light paths are considered bound within the waveguide, and are called modes. An optical waveguide can only support a finite number of bound modes. Each mode consists of two distinct parts, that which exists within the core of the waveguide (which is oscillatory in behaviour) and that part which travels along the interface of the core and cladding. The second part is called the evanescent wave, with an electric field amplitude that falls off exponentially with distance from the interface. A mode is identified by its' core and cladding mode parameters, U and W. U and W are related by the propagation constant  $\beta$ , which represents the component of the wavevector along the waveguide axis. If the wave has a wavenumber k, in free space, then in the core (medium with refractive index  $n_1$ , where  $n_1 > n_2$ ) its' value is  $n_1 k$ , so

$$\beta = n_1 k \cos \theta_z \quad \text{Eqn 1.1.2}$$

where  $\theta_z$  is the angle the wavevector makes with the waveguide axis (z axis)

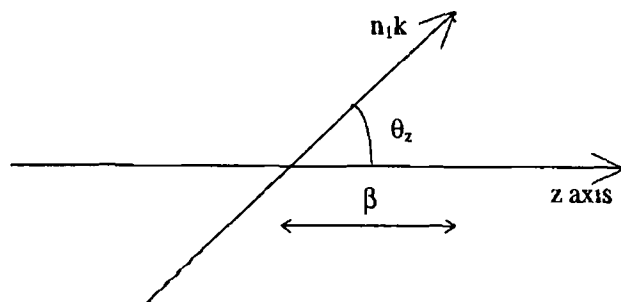


Figure 1-1 The propagation constant  $\beta$  of a particular mode

The transverse component is therefore

$$\sqrt{n_1^2 k^2 - \beta^2}$$

For a core dimension of  $2a$ , the core and cladding mode parameters are given by

$$U = a\sqrt{n_1^2 k^2 - \beta^2} \quad \text{Eqn 1 1 3}$$

$$W = a\sqrt{\beta^2 - n_2^2 k^2}$$

$U$  and  $W$  combine to give

$$U^2 + W^2 = a^2 k^2 (n_1^2 - n_2^2)$$

This is usually denoted

$$U^2 + W^2 = V^2$$

$$V = ak\sqrt{n_1^2 - n_2^2} \quad \text{Eqn 1 1 4}$$

$V$  is called the normalized frequency of a waveguide, and relates the core diameter ( $2a$ ) to the numerical aperture,  $NA = (n_1^2 - n_2^2)^{1/2}$ , and the wavenumber  $k$  of the light.  $V$  is a property only of the waveguide and of wavelength,  $\lambda$ . Because of the above equation,

$$0 \leq U \leq V$$

$$0 \leq W \leq V \quad \text{Eqn 1 1 5}$$

and when one is large, the other is small

## 1.2 The Planar Waveguide.

Figure 1-2 shows a planar waveguide

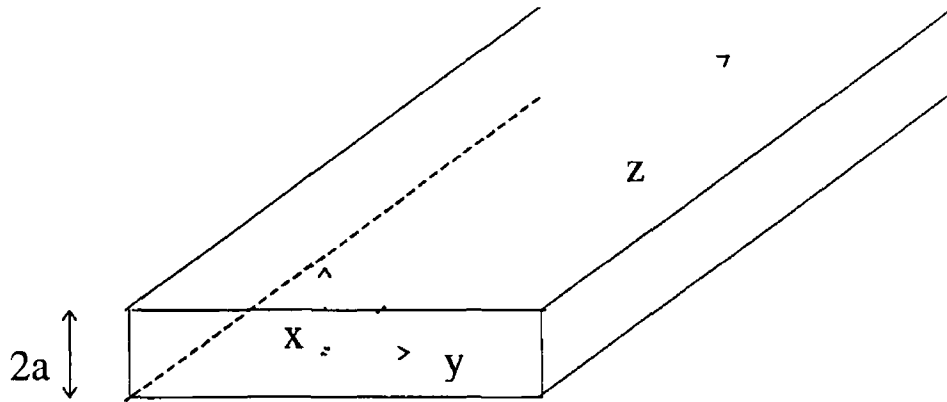


Figure 1 2 A Planar Waveguide

The solution to this waveguide is derived from the wave equation (equation 1 1 1) and is

$$\frac{\partial^2 E}{\partial x^2} + \frac{\partial^2 E}{\partial y^2} + \frac{\partial^2 E}{\partial z^2} - \frac{n^2}{c^2} \frac{\partial^2 E}{\partial t^2} = 0 \quad \text{Eqn 1 2 1}$$

in cartesian coordinates. Assuming that the E and H field components of the electromagnetic wave have a time (t) and distance (z) dependence of the form

$$\exp i(\omega t - \beta z) \quad \text{Eqn 1 2 2}$$

then a trial solution of

$$E = E_x \exp i(\omega t - \beta z) \quad \text{Eqn 1 2 3}$$

will yield the wave equation in the core and cladding as

$$\begin{aligned} a^2 \frac{\partial^2 E_x}{\partial x^2} + U^2 E_x &= 0 \quad @ \quad x \leq a \\ a^2 \frac{\partial^2 E_x}{\partial x^2} - W^2 E_x &= 0 \quad @ \quad x \geq a \end{aligned} \quad \text{Eqn 1 2 4}$$

U and W, the mode core and cladding parameters are given in section 1 1. The wavenumber k is given by  $2\pi/\lambda$ ,  $\lambda$  being the free space wavelength. The solutions to the above equations are given by

$$\begin{aligned}
 & \left. \begin{aligned} E &= A_1 \sin\left(\frac{Ux}{a}\right) \quad \text{or} \\ E &= A_2 \cos\left(\frac{Ux}{a}\right) \end{aligned} \right\} \text{for } x \leq a \\
 & E = A_3 \exp\left(-\frac{Wx}{a}\right) \quad \text{for } x \geq a
 \end{aligned}
 \tag{Eqn 1.2.5}$$

where  $A_1$ ,  $A_2$  and  $A_3$  are amplitude coefficients. Within the planar waveguide core the waves are sinusoidal (or cosinusoidal), and are evanescent in the cladding.

### 1.3 The Cylindrical Waveguide.

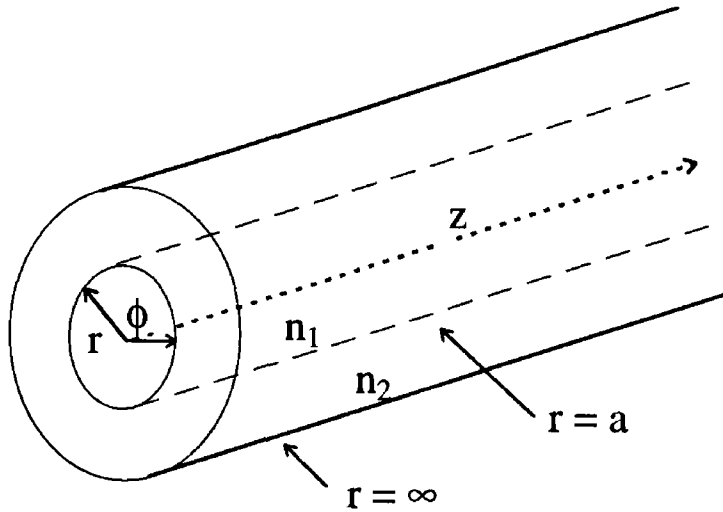


Figure 1.3 Cylindrical Waveguide

The cylindrical waveguide is shown in figure 1-3. The solution of the wave equation in a cylindrical waveguide is derived as follows:

$$\nabla^2 E - \frac{1}{v_p^2} \frac{\partial^2 E}{\partial t^2} = 0
 \tag{Eqn 1.3.1}$$

or

$$\nabla^2 E - \frac{n^2 k^2}{c^2} \frac{\partial^2 E}{\partial t^2} = 0
 \tag{Eqn 1.3.2}$$

where  $k = 2\pi/\lambda$ , and  $\lambda$  is the free space wavelength.

Expressing equation 1.3.1 in cylindrical polar coordinates  $(r, \phi, z)$  and inserting a trial solution of

$$\begin{aligned} E &= E(r, \phi) \exp i(\omega t - \beta z) \\ &= E_r \exp i(\omega t - \beta z) \end{aligned} \quad \text{Eqn 1.3.3}$$

gives

$$\frac{\partial^2 E_r}{\partial r^2} + \frac{1}{r} \frac{\partial E_r}{\partial r} + \frac{1}{r^2} \frac{\partial^2 E_r}{\partial \phi^2} + (n^2 k^2 - \beta^2) E_r = 0 \quad \text{Eqn 1.3.4}$$

Changing to a normalised radius  $R = r/a$  gives

$$\frac{\partial^2 E_r}{\partial R^2} + \frac{1}{R} \frac{\partial E_r}{\partial R} + \frac{1}{R^2} \frac{\partial^2 E_r}{\partial \phi^2} + a^2 (n^2 k^2 - \beta^2) E_r = 0 \quad \text{Eqn 1.3.5}$$

Since the medium has cylindrical symmetry we can write

$$E_r = F(R) \Phi(\phi) \quad \text{Eqn 1.3.6}$$

i.e. separating  $E_r$  in radial ( $R$ ) and azimuthal ( $\phi$ ) components Equation 1.3.5 then gives

$$\frac{R^2}{F} \left\{ \frac{d^2 F}{dR^2} + \frac{1}{R} \frac{dF}{dR} \right\} + R^2 (n^2 k^2 - \beta^2) = -\frac{1}{\Phi} \frac{d^2 \Phi}{d\phi^2} \quad \text{Eqn 1.3.7}$$

If we write equation 1.3.7 as some positive quantity  $+l^2$  then

$$-\frac{1}{\Phi} \frac{d^2 \Phi}{d\phi^2} = l^2 \quad \text{Eqn 1.3.8}$$

which has (S H M) solutions of the form  $\cos l\phi$  or  $\sin l\phi$ . For the function to be single valued, i.e.

$$\Phi(\phi) = \Phi(\phi + 2\pi) \quad \text{Eqn 1.3.9}$$

we must have  $l = 0, 1, 2, 3, \dots$ . Since for each value of  $l$  there may be two independent states of polarisation, modes with  $l \geq 1$  are four fold degenerate while  $l = 0$  modes, being  $\phi$  independent are two fold degenerate. In equation 1.3.7 above the second term  $R^2 (n^2 k^2 - \beta^2)$  may be positive or negative depending on the relative magnitude of  $nk$  and  $\beta$ .

a) When  $n^2 k^2 > \beta^2 > n^2 k^2$

For  $\beta$  in this range the radial fields  $F(R)$  are oscillatory in the core and decay in the cladding (evanescent). These are known as guided modes or bound modes. Recalling that  $\beta$  represents the  $z$  component of the wavevector  $n_1 k$  in the core, Snell's Law for rays says that guided or internally reflected rays occur if

$$\begin{aligned}\theta &> \sin^{-1} \frac{n_2}{n_1} \\ n_1 \sin \theta &> n_2 \\ n_1 k \sin \theta &> n_2 k\end{aligned}\tag{Eqn 1.3.10}$$

Where  $\theta$  is the angle the ray makes with the normal at the interface. Now  $\theta + \theta_z = \pi/2$  therefore Snell's Law gives

$$\begin{aligned}n_1 k \cos \theta_z &> n_2 k \\ \text{i.e. } \beta &> n_2 k\end{aligned}\tag{Eqn 1.3.11}$$

for total internal reflection. Since  $\beta = n_1 k \cos \theta_z$ ,  $\beta_{\max}$  is  $n_1 k$  so we have

$$n_1 k > \beta > n_2 k\tag{Eqn 1.3.12}$$

for total internal reflection ( $\theta_z$  is shown in Figure 1-1)

$$\text{b) } \beta^2 < n_2^2 k^2$$

For such values of  $\beta$  the radial fields  $F(R)$  are oscillatory in the cladding. These are known as radiation modes and correspond to refracted light in the cladding.

Returning to equation 1.3.7 the wave equation for guided or bound modes becomes

$$\begin{aligned}R^2 \frac{d^2 F}{dR^2} + R \frac{dF}{dR} + (U^2 R^2 - l^2) F &= 0 & R < 1 \\ R^2 \frac{d^2 F}{dR^2} + R \frac{dF}{dR} - (W^2 R^2 + l^2) F &= 0 & R > 1\end{aligned}\tag{Eqn 1.3.13}$$

where

$$\begin{aligned}U^2 &= a^2 (n_1^2 k^2 - \beta^2) \\ W^2 &= a^2 (\beta^2 - n_2^2 k^2)\end{aligned}\tag{Eqn 1.3.14}$$



Equations 1.3.13 are of the standard form of Bessel Equations with solution  $J_l(UR)$ ,  $Y_l(UR)$  in the  $R < 1$  core region and modified Bessel functions  $K_l(WR)$  and  $I_l(WR)$  in the cladding

The equations above give the allowed solutions

$$\left. \begin{aligned} E_t &= A_1 J_l(UR) \cos(l\phi) \\ \text{or } E_t &= A_1 J_l(UR) \sin(l\phi) \end{aligned} \right\} \text{for } R \leq 1$$

$$\left. \begin{aligned} E_t &= A_1 K_l(WR) \cos(l\phi) \\ \text{or } E_t &= A_1 K_l(WR) \sin(l\phi) \end{aligned} \right\} \text{for } R \geq 1$$

Eqn 1.3.15

where  $A_1$  is the wave amplitude. The  $Y_l(UR)$  and  $I_l(WR)$  Bessel functions are not allowed solutions in this case as  $Y_l(UR)$  is infinite at  $R = 0$ , and  $I_l(WR)$  is infinite at  $R = \infty$  (Abramowitz and Stegun, Figures 9.1 and 9.8)

## 1.4 The Evanescent Power Fraction.

For both planar and cylindrical waveguides the evanescent field

- (i) is approximately exponentially decaying away from the interface
- (ii) Has a penetration depth  $\cong a/W$ , or

$$d_p \approx \frac{1}{\sqrt{\beta^2 - n_2^2 k^2}}$$

By taking the Poynting vector ( $\vec{E} \times \vec{H}$ ) and integrating from  $R = 1$  to  $R = \infty$ , the power of the evanescent wave may be calculated. Thus the power fraction of a mode which exists as an evanescent wave can be determined. This fraction  $f$ , was shown by Gloge (1971) to be

$$f \approx \frac{U^2}{V^2 \sqrt{W^2 + l^2 + 1}}$$

Eqn 1.4.1

For modes close to cut-off, i.e. modes for which  $W \rightarrow 0$ , this fraction will be large, ( $W \rightarrow 0$  as  $U \rightarrow V$ )

$$f \equiv 1/l$$

while for modes far from cutoff ( $W \rightarrow V$ , as  $U \rightarrow 0$ ) the power fraction will be negligible

### ***1.5 The Waveguide as a Sensor.***

In order for a waveguide to be used as a sensor, an analytical wavelength of the cladding material must match that of the light being carried by the core. The cladding will then absorb photons from the modes at a rate determined by the bulk absorption coefficient of the cladding material (which may be solid or fluid). The amount of absorption that occurs also depends on the distance over which the core is in contact with the absorbing medium. The sensing mechanism is the detection of the size of this power loss into the absorber, and relating the power loss to the concentration of absorber present. Various evanescent wave sensor geometries are possible. Harrick (1987) Chapter 4 discusses rectangular waveguide designs. Kapany et al (1963) I and II, Hansen (1963) and Harrick (1964) describe solid rod waveguides used in attenuated wave spectrophotometry.

## 1.6 Absorbance of a Sensor Probe.

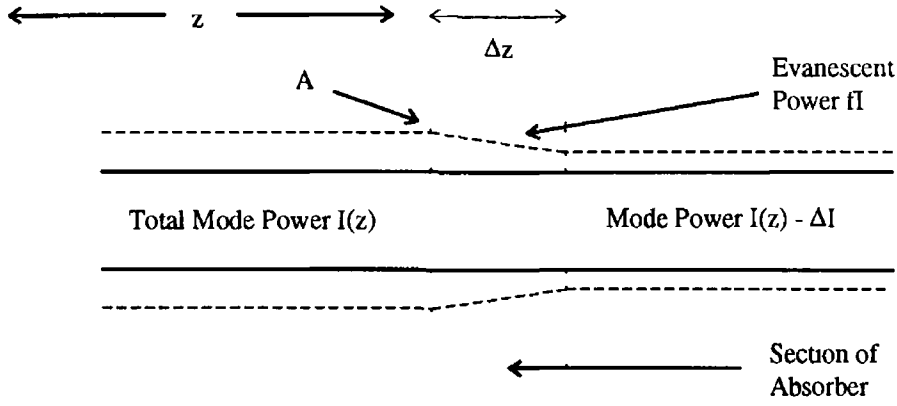


Figure 1-4 Power distribution in a waveguide

Because only light being transmitted as an evanescent wave comes in contact with the absorber, only a small fraction of the total light launched into the waveguide is used to provide sensor information. Therefore a modified version of the Lambert-Beer law applies, being

$$I = I_0 \exp(-f\alpha z) \quad \text{Eqn 1.6.1}$$

This can be seen as follows. The evanescent power at point A in Figure 1.4 is

$$I(z) = fI \quad \text{Eqn 1.6.2}$$

The loss in power of the mode in travelling  $\Delta z$  is  $\Delta I$ , where

$$\frac{\Delta I}{I(z)} = -\alpha(\Delta z) \quad \text{Eqn 1.6.3}$$

Using equation 1.6.2 gives

$$\frac{\Delta I}{I} = -f\alpha \Delta z \quad \text{Eqn 1.6.4}$$

On integrating from  $z = 0$  to  $z$ , for  $I = I_0$  to  $I$  we get

$$\log \frac{I}{I_0} = -f\alpha z \quad \text{Eqn 1.6.5}$$

i e

$$I = I_0 \exp(-\alpha f z) \quad \text{Eqn 1 6 6}$$

$$A' = (0.434) f \alpha z \quad \text{Eqn 1 6 7}$$

For a given mode, specified by the core mode parameter U, and cladding mode parameter W, then the above equation gives the evanescent absorbance A' using equation 1 4 1 for f - as

$$A' = (0.434) \frac{U^2 \alpha z}{V^2 \sqrt{W^2 + l^2 + 1}} \quad \text{Eqn 1 6 8}$$

In this case z is the length of the waveguide in contact with the absorber. Where many modes are excited, each with the same incident power ( $I_0 / N$ ), the transmitted power will be

$$I = \sum_N \left( \frac{I_0}{N} \right) \exp \left\{ \frac{-U^2 \alpha z}{V^2 \sqrt{W^2 + l^2 + 1}} \right\} \quad \text{Eqn 1 6 9}$$

$$I/I_0 = \frac{1}{N} \sum_N \exp \left\{ \frac{-U^2 \alpha z}{\sqrt{W^2 + l^2 + 1}} \right\} \quad \text{Eqn 1 6 10}$$

$$A' = -\log_{10} \left[ \frac{1}{N} \sum_N \exp \left\{ \frac{\alpha z U^2}{\sqrt{W^2 + l^2 + 1}} \right\} \right] \quad \text{Eqn 1 6 11}$$

where the summation is carried out over N modes. A' is the evanescent absorbance

## 1.7 Conclusions.

This chapter provides the basis from which theoretical analysis on the hollow cylindrical waveguide will be done. The methods shown above will be expanded to describe the hollow waveguide in similar mathematical terms, so that the hollow waveguide will describe both the planar and fibre waveguides when the dimensions of the hollow waveguide are sufficiently large to be considered planar or small enough to be considered a solid fibre.

## **1.8 References.**

- Abramowitz M** and **Stegun I A**, "Handbook of Mathematical Functions", (National Bureau of Standards, Washington DC USA 1964) Eqn 9-5-28 p374
- Gloge D**, "Weakly Guiding Fibers", *Appl Opt* 10 pp 2252 - 2258 (1971)
- Hansen W N**, "A New Spectrophotometric Technique using Multiple Attenuated Total Reflection", *Anal Chem* 35 765-769 (1963)
- Harrick N J**, "Multiple Reflection Cells for Internal Reflection Spectroscopy", *Anal Chem* 36 188-193 (1964)
- Harrick N J**, "Internal Reflection Spectroscopy", (Harrick Scientific Corp NY (1987))
- Kapany N S** and **Pontarelli D A (I)**, "Photorefractometer I Extension of Sensitivity and Range", *Appl Opt* 2 425-430 (1963)
- Kapany N S** and **Pontarelli D A (II)**, "Measurement of N and K", *Appl Opt* 2 1043-1050 (1963)
- Snyder A W** and **Love J D**, "Optical Waveguide Theory", (Chapman and Hall, London / NY (1983))

## 2. The hollow cylindrical waveguide - a theoretical mode analysis.

### 2.1 Introduction.

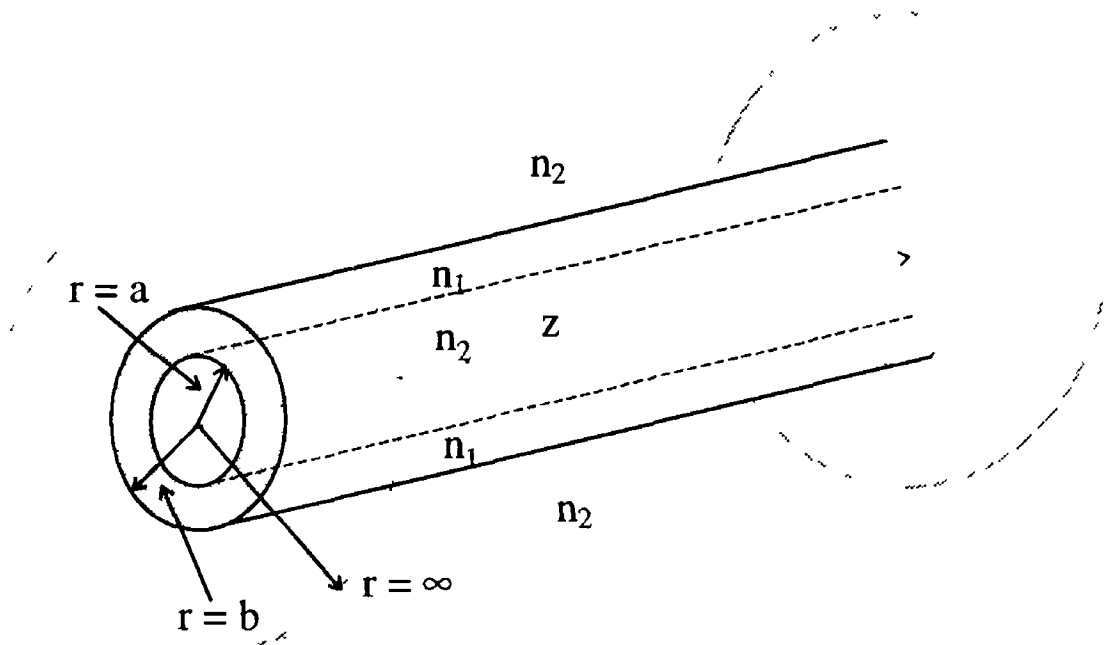


Figure 2 1 Hollow cylindrical waveguide

Figure 2-1 above shows a hollow cylindrical waveguide. The inner hole ( $0 < r < a$ ) and outer region ( $b < r < \infty$ ) are the lower index media, and the glass region  $a < r < b$  is the higher refractive index medium. In this configuration the glass annulus acts as a light guide, but with cladding at two interfaces giving two surfaces where evanescent absorption can take place.

### 2.2 The E and H fields of modes in a hollow waveguide.

The hollow cylinder is described as having an inner diameter of  $2a$  and outer diameter  $2b$ , this region being made of a glass with refractive index  $n_1$ , and surrounded internally and externally by a medium of refractive index  $n_2$  with  $n_1 > n_2$ . The following analysis is based on the method used in

Unger(1980) for E and H fields in doubly clad cylindrical fibre waveguides modified for the hollow cylinder

Barlow (1981, 1983) developed the first published work on the “three concentric layer cylindrical waveguide” In his analysis - pertaining to fiber waveguides - the waveguide dimensions are small (typically 100  $\mu\text{m}$ ) and the refractive indices of the 3 layers ( $n_1, n_2, n_3$ ) are very close together, obeying the so-called “weakly guiding approximation” The latter condition is valid only in very limited cases but the thrust of the mode analysis can form a basis for a more general theory Tsao et al (1989) carried out further 3 layer fiber mode characterisations, again invoking a weakly guiding condition Brunner et al (1995) published some work on Attenuated Total Reflection Spectrophotometry using “capillary optical fiber” probes using the mode analysis technique of Barlow (1983) for their work Mode analysis for a 3 layered cylindrical waveguide of a hollow cylinder shape, where the guiding glass annulus is surrounded by 2 media of the same refractive index (as shown in figure 2 1) is carried out by the author without recourse to the weakly guiding condition ( $n_1 \approx n_2$ ) This is the most general case and the analysis described here is the first representation of such a treatment

Solutions of the wave equations in a medium in which the phase velocity of light is  $v = c/n$

$$\begin{aligned}\bar{\nabla}^2 \bar{E} - \frac{1}{v^2} \frac{\partial \bar{E}}{\partial t^2} &= 0 \\ \bar{\nabla}^2 \bar{H} - \frac{1}{v^2} \frac{\partial \bar{H}}{\partial t^2} &= 0\end{aligned}\tag{Eqn 2 2 1}$$

(where  $\bar{\nabla}^2$  is a vector operator) may be expressed in terms of the two waveguide parameters U and W, defined in equation 1 1 3 The two vector differentials 2 2 1 for E and H can be broken into six differential scalar equations Of these, four involve more than one E or H field component The other two involve the z components  $E_z$  or  $H_z$  alone These can be written as

$$\left\{ \frac{\partial^2}{\partial R^2} + \frac{1}{R} \frac{\partial}{\partial R} + \frac{1}{R^2} \frac{\partial^2}{\partial \phi^2} + U^2 \right\} E_z = 0 \quad @ 1 < R < C$$

$$\left\{ \frac{\partial^2}{\partial R^2} + \frac{1}{R} \frac{\partial}{\partial R} + \frac{1}{R^2} \frac{\partial^2}{\partial \phi^2} - W^2 \right\} E_z = 0 \quad @ \begin{cases} 0 < R < 1 \\ C < R < \infty \end{cases} \quad \text{Eqn 2 2 2}$$

where  $R$  is the normalised radius  $r/a$  and  $C$  is given by  $b/a$ . The  $\phi$  dependence of the fields may be represented by  $\cos l\phi$  or  $\sin l\phi$  terms giving a degeneracy of four for  $l > 0$  in general and a degeneracy of two - corresponding to only two orthogonal polarisations - for the  $l = 0$  modes. Similar equations can be written for the  $H_z$  fields

The solutions of these equations in the three zones of interest, (within the centre of the tube, the glass itself and outside the tube) ignoring those whose values become infinite at any of the boundaries ( $R = 0$ ,  $R = 1$ ,  $R = \infty$ ) are

$$\begin{aligned} I_l(WR) \cos(l\phi) \\ I_l(WR) \sin(l\phi) \end{aligned} \quad \text{in } 0 \leq R \leq 1 \quad \text{Eqn 2 2 3}$$

$$\begin{aligned} J_l(UR) \cos(l\phi) \text{ and } Y_l(UR) \cos(l\phi) \\ J_l(UR) \sin(l\phi) \text{ and } Y_l(UR) \sin(l\phi) \end{aligned} \quad \text{in } 1 \leq R \leq C \quad \text{Eqn 2 2 4}$$

$$\begin{aligned} K_l(WR) \cos(l\phi) \\ K_l(WR) \sin(l\phi) \end{aligned} \quad \text{in } C \leq R \leq \infty \quad \text{Eqn 2 2 5}$$

where  $J_l$  and  $K_l$  are Bessel functions of the first and second kind (of order  $l$ ) and represent oscillatory functions,  $I_l$  and  $Y_l$  are modified Bessel functions of the first and second kind and represent exponentially varying functions of  $R$ , respectively (Abramowitz and Stegun, 1964). If each field is normalised so that it is unity in the  $R = 1$  interface, the fields of the even modes in the glass can be written

$$\begin{aligned} E_z &= i(A + B) \frac{I_l(WR)}{I_l(W)} \cos l\phi & R < 1 \\ E_z &= i \left\{ A \frac{J_l(UR)}{J_l(U)} + B \frac{Y_l(UR)}{Y_l(U)} \right\} \cos l\phi & 1 < R < C \\ E_z &= iE \frac{K_l(WR)}{K_l(W)} \cos l\phi & C < R \end{aligned} \quad \text{Eqn 2 2 6}$$



with the  $H_z$  fields as

$$\begin{aligned}
 H_z &= \iota(G + D) \frac{I_l(WR)}{I_l(W)} \sin l\phi & R < 1 \\
 H_z &= \iota \left\{ G \frac{J_l(UR)}{J_l(U)} + D \frac{Y_l(UR)}{Y_l(U)} \right\} \sin l\phi & 1 < R < C \\
 H_z &= \iota F \frac{K_l(WR)}{K_l(W)} \sin l\phi & C < R
 \end{aligned} \tag{Eqn 2.2.7}$$

In equations 2.2.5 and 2.2.6 above the constants A, B, G, D, E, F represent six field amplitudes. The Bessel functions are normalised to have unit values at the inner interface  $R = 1$ .  $E_z$  and  $H_z$  are chosen to be imaginary in order that the transverse components  $E_r$ ,  $E_\phi$  and  $H_r$ ,  $H_\phi$  are real. The radial and azimuthal (transverse) fields can be derived from the axial (i.e.  $z$ ) field components using the well known relationships (Snyder and Love, 1983)

$$\begin{aligned}
 E_r &= \frac{\iota}{a(n^2 k^2 - \beta^2)} \left\{ \beta \frac{\partial E_z}{\partial R} + \frac{kZ}{R} \frac{\partial H_z}{\partial \phi} \right\} \\
 H_r &= \frac{\iota}{a(n^2 k^2 - \beta^2)} \left\{ \beta \frac{\partial H_z}{\partial R} - \frac{n^2 k}{ZR} \frac{\partial E_z}{\partial \phi} \right\} \\
 E_\phi &= \frac{\iota}{a(n^2 k^2 - \beta^2)} \left\{ \frac{\beta}{R} \frac{\partial E_z}{\partial \phi} - kZ \frac{\partial H_z}{\partial R} \right\} \\
 H_\phi &= \frac{\iota}{a(n^2 k^2 - \beta^2)} \left\{ \frac{\beta}{R} \frac{\partial H_z}{\partial \phi} + \frac{n^2 k}{Z} \frac{\partial E_z}{\partial R} \right\}
 \end{aligned} \tag{Eqn 2.2.8}$$

where  $Z^2 = (\mu_0/\epsilon_0)$  is the characteristic impedance of free space squared. Differentiation of equations 2.2.5 and 2.2.6 allow the  $E_r$ ,  $H_r$ ,  $E_\phi$  and  $H_\phi$  field components to be evaluated in all three zones of the waveguide in terms of the various Bessel functions, their first derivatives (Snyder and Love, 1983) with respect to  $R$ , the mode parameters  $U$  and  $W$  and the 6 amplitude coefficients A - F.

### 2.3 The mode eigenvalue equation.

The six field components  $e_z$ ,  $e_\phi$ ,  $e_r$ ,  $h_z$ ,  $h_\phi$ ,  $h_r$  in each of the three zones ( $0 < R < 1$ ,  $1 < R < C$ ,  $R > C$ ) were determined. These are listed in Appendix A. The continuity of the field components at

the two interfaces  $R = 1$  and  $R = C$  generate a set of equations, the solutions of which give the allowed values of the parameters  $U$  and  $W$  (or the allowed values of the propagation constant  $\beta$ )

The solutions of these six equations were obtained by placing them in a matrix, and calculating the determinant of the matrix. The equations used to form the determinant are as follows, with the prime indicating differentiation with respect to the argument

$$A \frac{J_l(UC)}{J_l(U)} + B \frac{Y_l(UC)}{Y_l(U)} - E \frac{K_l(WC)}{K_l(W)} = 0 \quad e_z \text{ at } R = C \quad \text{Eqn 2 3 1}$$

$$G \frac{J_l(UC)}{J_l(U)} + D \frac{Y_l(UC)}{Y_l(U)} - F \frac{K_l(WC)}{K_l(W)} = 0 \quad h_z \text{ at } R = C \quad \text{Eqn 2 3 2}$$

$$\begin{aligned} & -A\beta l \left( \frac{1}{U^2} + \frac{1}{W^2} \right) - B\beta l \left( \frac{1}{U^2} + \frac{1}{W^2} \right) + \\ & G \left\{ \frac{p}{W} \frac{I'_l(W)}{I_l(W)} + \frac{p}{U} \frac{J'_l(U)}{J_l(U)} \right\} + D \left\{ \frac{p}{W} \frac{I'_l(W)}{I_l(W)} + \frac{p}{U} \frac{Y'_l(U)}{Y_l(U)} \right\} = 0 \end{aligned}$$

$e_\phi \text{ at } R = 1 \quad \text{Eqn 2 3 3}$

$$\begin{aligned} & A \left\{ \frac{qn_2^2}{W} \frac{I'_l(W)}{I_l(W)} + \frac{qn_1^2}{U} \frac{J'_l(U)}{J_l(U)} \right\} + B \left\{ \frac{qn_2^2}{W} \frac{I'_l(W)}{I_l(W)} + \frac{qn_1^2}{U} \frac{Y'_l(U)}{Y_l(U)} \right\} \\ & + G\beta l \left( \frac{1}{U^2} + \frac{1}{W^2} \right) + D\beta l \left( \frac{1}{U^2} + \frac{1}{W^2} \right) = 0 \end{aligned}$$

$h_\phi \text{ at } R = 1 \quad \text{Eqn 2 3 4}$

$$\begin{aligned} & A \frac{\beta l}{U^2 C} \frac{J_l(UC)}{J_l(U)} + B \frac{\beta l}{U^2 C} \frac{Y_l(UC)}{Y_l(U)} - G \frac{p}{U} \frac{J'_l(UC)}{J_l(U)} \\ & - D \frac{p}{U} \frac{Y'_l(UC)}{Y_l(U)} + E \frac{\beta l}{W^2 C} \frac{K_l(WC)}{K_l(W)} - F \frac{p}{W} \frac{K'_l(WC)}{K_l(W)} = 0 \end{aligned}$$

$e_\phi \text{ at } R = C \quad \text{Eqn 2 3 5}$

$$\begin{aligned} & -A \frac{qn_1^2}{U} \frac{J'_l(UC)}{J_l(U)} - B \frac{qn_1^2}{U} \frac{Y'_l(UC)}{Y_l(U)} - G \frac{\beta l}{U^2 C} \frac{J_l(UC)}{J_l(U)} \\ & - D \frac{\beta l}{U^2 C} \frac{Y_l(UC)}{Y_l(U)} - E \frac{qn_2^2}{W} \frac{K'_l(WC)}{K_l(W)} - F \frac{\beta l}{W^2 C} \frac{K_l(WC)}{K_l(W)} = 0 \end{aligned}$$

$h_\phi \text{ at } R = C \quad \text{Eqn 2 3 6}$

Each pair of  $U$  and  $W$  values (same  $\beta$  value) that allow the value of the determinant to be zero (for a range of  $l$  values) is considered to be a valid solution, and therefore an allowed mode, provided it also meets the cut-off condition (which is discussed in section 2.4)

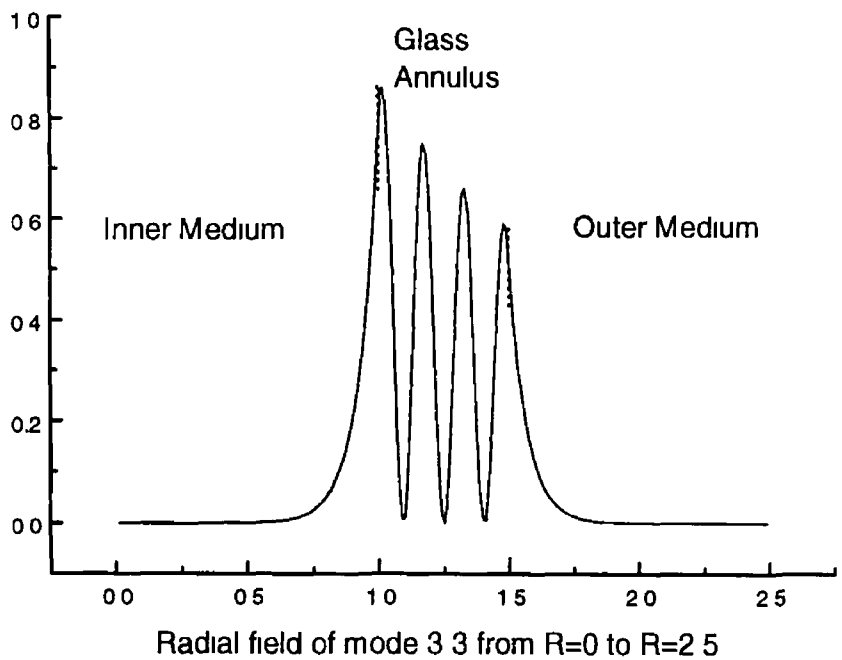


Figure 2-2 Radial E field of (3, 3) mode

A computationally generated radial field for the (3, 3) mode is shown in figure 2-2. The continuity of  $E_r$  at both interfaces  $R = 1$  (i.e.  $r = a$ ) and  $R = C$  (i.e.  $r = b$ ) may be seen. Figure 2-3 shows the radial E field of the (1, 3) mode in the annulus only (from  $R = 1$  to 1.5). It can be seen from the graph that there are two sets of intensity maxima, each  $180^\circ$  degrees apart, and lessening in intensity as the distance from the centre of the annulus increases. The number of intensity maxima in each row was found to be equal to  $(l + 1)$ , and the number of rows was found to be equal to  $(2m)$ .

### Mode 1,3 Intensity Plot

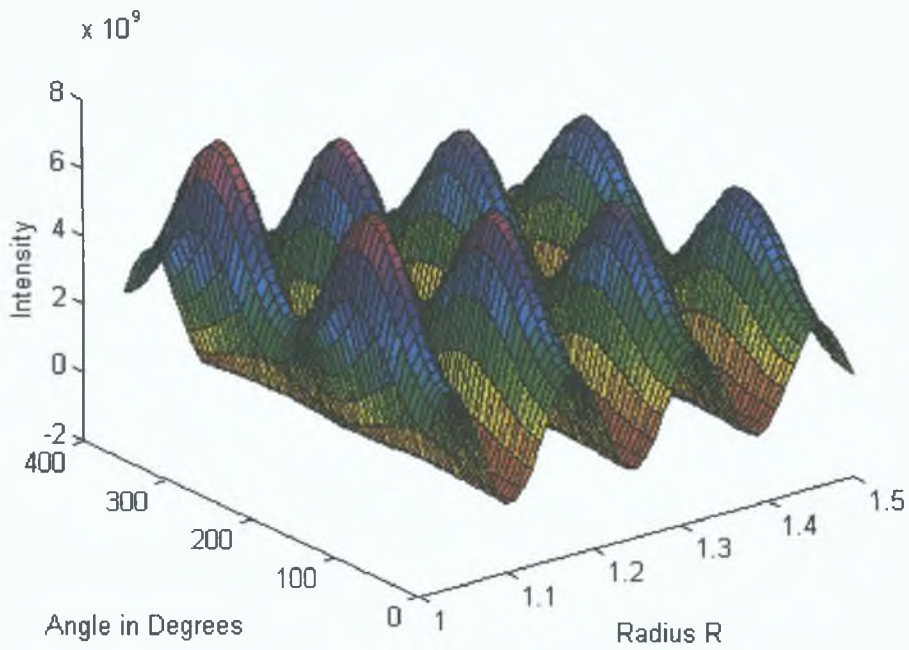


Figure 2-3: Radial E field in three dimensions.

## 2.4 Mode cut-off condition.

A mode is considered to be cut-off when  $W = 0$  ( $\beta = n_2 k$ ). Applying this condition to the six by six determinant gives line 1 as

$$A \frac{J_1(UC)}{J_1(U)} + B \frac{Y_1(UC)}{Y_1(U)} = 0 \quad \text{Eqn 2.4.1}$$

( $K_1(0) \rightarrow \infty$ )

likewise line 2 gives

$$G \frac{J_1(UC)}{J_1(U)} + D \frac{Y_1(UC)}{Y_1(U)} = 0 \quad \text{Eqn 2.4.2}$$

Multiplying line 3 by  $W^2$  gives

$$\begin{aligned} -\beta l A - \beta l B &= 0 \\ \Rightarrow A + B &= 0 \end{aligned}$$

*Eqn 2 4 3*

Similarly line 4 by  $W^2$  gives

$$\begin{aligned} \beta l G + \beta l D &= 0 \\ \Rightarrow G + D &= 0 \end{aligned}$$

*Eqn 2 4 4*

Multiplying line 5 by  $W^2$  gives

$$E = 0$$

*Eqn 2 4 5*

And line 6 by  $W^2$  gives

$$F = 0$$

*Eqn 2 4 6*

The solution of equations 2 4 1 and 2 4 3 give the cut-off condition

$$\begin{aligned} \left| \begin{array}{cc} \frac{J_l(UC)}{J_l(U)} & \frac{Y_l(UC)}{Y_l(U)} \\ 1 & 1 \end{array} \right| &= 0 \\ \text{or } J_l(UC)Y_l(U) - Y_l(UC)J_l(U) &= 0 \end{aligned}$$

*Eqn 2 4 7*

For each integer value of  $l$  (0, 1, 2 ...) the above equation has many roots, which are specified by  $m = 1, 2, 3$  ... Thus an array of  $U$  values indexed by  $l$  and  $m$  ( $U_{l,m}$ ) mode can be created

Each member of the family of  $(U_{l,m})_{\text{cut-off}}$  values is the lowest possible value for a solution to the six by six determinant for its' given  $(l, m)$  values

$$U_{l,m} > (U_{l,m})_{\text{cut-off}}$$

*Eqn 2 4 8*

Since the maximum value of  $U$  is  $V$  (the  $V$  number of the waveguide) at which  $W = 0$ , the cut-off condition for the  $(l, m)$  mode becomes

$$J_l(VC)Y_l(V) - Y_l(VC)J_l(V) = 0$$

*Eqn 2 4 9*

Solutions to the above equation are given in Abramowitz and Stegun (1964), equation 9-5-28, page 374 as

$$V = (U_{l,m})_c \equiv \beta + \frac{p}{\beta} + \frac{q - p^2}{\beta^3} + \frac{e + 4pq - 2p^3}{\beta^5} +$$

*Eqn 2 4 10*

where  $\beta = m\pi/C - 1$

$$\mu = 4l^2$$

$$p = (\mu - 1) / 8C$$

$$q = (\mu - 1) (\mu - 25) (C^3 - 1) / 384C^3 (C - 1)$$

$$r = (\mu - 1) (\mu^2 - 114\mu + 1073) (C^5 - 1) / 5120C^5 (C - 1)$$

( $\beta$  above is not the propagation constant defined earlier in equation 1 1 2)

Equation 2 4 10 is valid only for  $\beta \gg p / \beta$  or

$$m \gg l^{\frac{2}{3}} \left( \frac{C - 1}{2\pi C^{\frac{1}{3}}} \right) \quad \text{Eqn 2 4 11}$$

## 2.5 Mode indices ( $l, m$ ).

For the fundamental mode ( $l = 0, m = 1$ ) single mode operation exists for  $V = 12.6$  with  $C = 1.25$  and for  $V = 6.27$  with  $C = 1.5$  ( $V < \pi / (C - 1)$  approximately) Equation 2 4 10 can be used to extract the maximum value of  $m$  for  $l = 0$  modes and yields the value

$$m_{\max} = \frac{(C - 1)}{\pi} V \quad \text{Eqn 2 5 1}$$

Expanding equation 2 4 10 to the second term yields a functional relationship between  $l$  and  $m$  of

$$El^2 + Fm + Gm^2 = 0 \quad \text{Eqn 2 5 2}$$

where  $E, F$  and  $G$  are functions of  $V$  and  $C$  ( $E = 4, F = 8\pi CV$  and  $G = 8\pi^2 C / (C - 1)$ ) For a large  $V$  number waveguide ( $V \gg 1$ ) the third term in equation 2 5 2 can be disregarded so that

$$El^2 + Fm = 0 \quad \text{Eqn 2 5 3}$$

i.e.  $l$  and  $m$  are related in a parabolic fashion for

$$m \gg l^{\frac{2}{3}} \left( \frac{C-1}{2\pi C^{\frac{1}{3}}} \right) \quad \text{Eqn 2.5.4}$$

For the other extreme, i.e. small  $m$  and large  $l$  the approximation of equation 2.4.10 no longer holds

Numerical modelling indicates that an equation of the form

$$m = Sl^2 + Tl + U \quad \text{Eqn 2.5.5}$$

applies, i.e. the  $m$  versus  $l$  graph is parabolic in shape ( $S$ ,  $T$  and  $U$  are constant for a particular waveguide). Furthermore the data generated for waveguides of different  $V$  and  $C$  values indicate that to a good approximation  $l_{\max}$  is given by

$$l_{\max} = \frac{2(C+1)V}{\pi} \quad \text{Eqn 2.5.6}$$

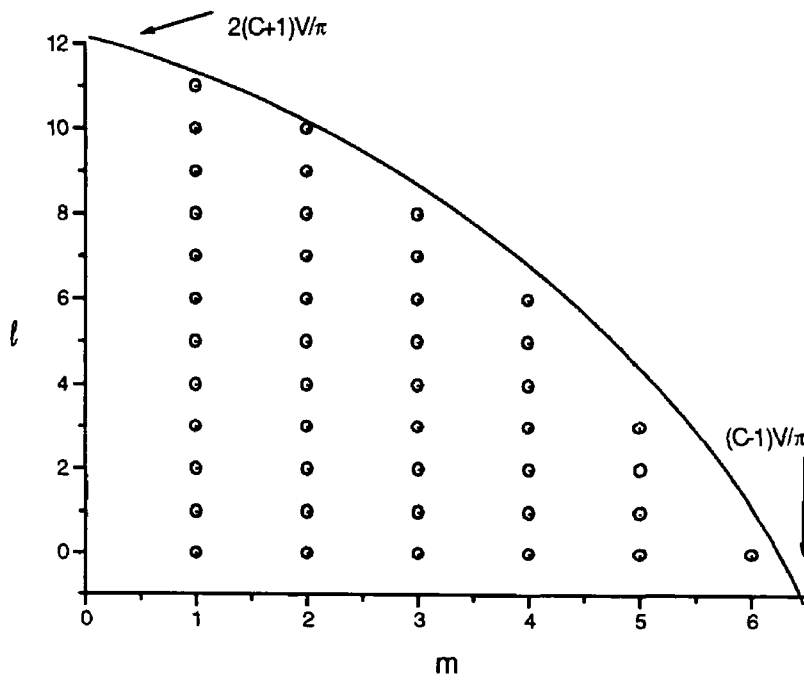


Figure 2.4 Example of  $l$  versus  $m$  graph

## 2.6 Limiting values of $l$ and $m$ .

The total number of (non-degenerate) modes is given by four times the area of the bounded region shown in figure 2-4. As the area of a parabola is

$$\frac{2}{3} x_{\max} y_{\max} \quad \text{Eqn 2.6.1}$$

the total number of bound modes in the waveguide ( $N$ ) is

$$N = 4 \times \frac{2}{3} \times \frac{2(C+1)}{\pi} V \times \frac{(C-1)}{\pi} V$$

*or*

$$N = 0.54(C^2 - 1)V^2 \quad \text{Eqn 2.6.2}$$

## 2.7 An effective $V$ number for the waveguide ( $V'$ ).

Substituting  $C = b/a$  and equation 1.1.4 into equation 2.6.2 gives

$$N = 0.54 \left( \frac{b^2}{a^2} - 1 \right) \left( ka \sqrt{n_1^2 - n_2^2} \right)^2$$

$$N \equiv \frac{V'^2}{2} \quad \text{Eqn 2.7.1}$$

where

$$V' = \frac{2\pi}{\lambda} \sqrt{n_1^2 - n_2^2} \sqrt{(b^2 - a^2)} \quad \text{Eqn 2.7.2}$$

In the limit  $a \rightarrow 0$   $V'$  reduces to the  $V$  number of the step index fibre waveguide of equation 1.1.4, and therefore the total number of modes  $N$  becomes  $V^2/2$ , which is predicted by Gloge, equation 36 (1971) for such a waveguide.  $V'$  is called the effective  $V$  number of the hollow cylindrical waveguide. This effective  $V$  number for the hollow cylindrical waveguide has not been reported to date. Tsao et al (1989) in their treatment of a 3 layered fiber structure derive an expression

$$\frac{2\pi}{\lambda} (b-a) \sqrt{n_1^2 - n_2^2} \quad \text{Eqn 2.7.3}$$

for its  $V$  number. This is significantly different to equation 2.7.2 especially when  $b \gg a$



## 2.8 Single mode operation.

The condition for  $m_{\max}$  given in equation 2.5.1 may be used to derive the condition for single mode operation of this waveguide. Putting  $m_{\max} = 1$  yields

$$\begin{aligned}
 (C-1)V &< \pi \\
 \text{or } \left(\frac{b}{a}-1\right)ka(NA) &< \pi \\
 \Rightarrow (b-a) &< \frac{\pi}{(k)NA} \\
 \Rightarrow (b-a) &< \frac{\lambda}{2NA}
 \end{aligned}
 \tag{Eqn 2.8.1}$$

i.e. if the waveguide thickness  $(b-a)$  is less than the light wavelength divided by twice the waveguide numerical aperture  $NA$  [ $NA^2 = n_1^2 - n_2^2$ ], only the fundamental  $(0, 1)$  mode can propagate in the waveguide. This condition is quoted by Tsao et al (1989) for single mode operation of what they refer to as a "Ring fibre waveguide" [Equation 9.123 of Tsao 1989]. This is referenced in Tsao (1992) which treats the three-layered cylindrical waveguide using Debye potentials. The field functions  $(E_r, E_\phi, E_z)$  and  $(H_r, H_\phi, H_z)$  obtained by Tsao (1992) are identical to those quoted in this analysis when his third layer refractive index  $n_3$  is equated to  $n_2$  in this analysis. The author was not aware of this paper when the enclosed analysis was carried out.

## 2.9 The evanescent power fraction of a mode.

The mode power in the  $z$  direction in all three zones in the waveguide may be obtained from the Poynting vector

$$P_z = \pi a^2 \int (E_r H_\phi - E_\phi H_r) R dR \tag{Eqn 2.9.1}$$

using the limits appropriate to the zone in question, i.e.  $(0, 1)$ ,  $(1, C)$  and  $(C, \infty)$  for the inner cladding, the core and the outer cladding, with the integration being made over the cross-sectional

area (The radial and azimuthal fields are given previously in equation 2.2.8) As the power ratios in the evanescent fields only are of interest, the factor of  $2\pi$  and

$$\int_0^{2\pi} \cos^2(l\phi) d\phi = \pi \quad \text{Eqn 2.9.2}$$

are ignored

## 2.10 The evanescent power fraction of a mode.

The evanescent power fraction of each mode within a waveguide may be calculated from

$$f_{lm} = \frac{[P_z]_{R=0}^l + [P_z]_{R=C}^\infty}{[P_z]_{R=0}^l + [P_z]_{R=1}^C + [P_z]_{R=C}^\infty} \quad \text{Eqn 2.10.1}$$

using equation 2.9.1 to evaluate  $P_z$ . Summing over  $l$  and  $m$  for all allowed modes within a waveguide, and dividing by the number of modes gives the average evanescent power fraction for a mode within a particular waveguide

## 2.11 Conclusions.

The above analysis shows that a hollow cylindrical waveguide can act as a light guide when that light travels in the allowed modes dictated by the eigenvalue equations and the boundary conditions. The core and cladding parameters  $U$  and  $W$  can be predicted for a waveguide of any given dimension for the equations discussed. The number of modes that can be sustained by the waveguide can also be predicted using the above theoretical derivations. The power distribution of core guided light to evanescently bound light can also be described for each mode in the hollow cylindrical waveguide.

## **2.12 References.**

**Barlow** H M, "A Large Diameter Optical Fiber Waveguide For Exclusive Transmission In The  $HE_{11}$  Mode", J Phys D Appl Phys 16 1539-1451 (1983)

**Barlow** H M, "A Cladded Tubular Glass-fiber Guide For Singlemode Transmission" J Phys D Appl Phys 14 405-412 (1981)

**Brunner** R, Doupouec J, Suchy F and Berta M, "Evanescent -wave Penetration Depth in Capillary Optical Fibers Challenges For The Liquid Sensing", Acta Physica Slovaca 45 (4) 491-498 (1995)

**Gloge** D, "Weakly Guiding Fibres", Applied Optics 10 pp2252 - 2258 (1971) Eqn 36

**Snyder** A W and Love J D "Optical Waveguide Theory", (Chapman & Hall (1983)) Eqn 30-9 p593

**Tsao** C, "Optical Fibre Waveguide Analysis", (Oxford University Press, NY (1992)), Section 9 2 pp 300 - 352

**Tsao** C Y H, Payne D N and Gambling W A, "Modal characteristics of three layered optical fibre waveguides a modified approach", J Opt Soc Am A, pp 555-563 (1989)

**Tsao** C Y H, Payne D N and Gambling W A, "Modal Characteristics of Three-Layered Optical Fiber Waveguides A Modified Approach", J Opt. Soc Am A 6 4, 555-563 (1989)

**Unger** H G, "Planar Optical Waveguides and Fibres", (Clarendon Press, Oxford (1980))

### **3. Model of hollow cylindrical waveguides - a computational analysis.**

#### **3.1 Introduction.**

This chapter describes the computational methods and computer programs used to create an accurate simulation of the bound modes in a hollow cylindrical waveguide probe. Each of the programs used was written in the Matlab language (which is based on matrices), and runs only in the Matlab environment. A program called *Modes m* was written to control the other programmes.

#### **3.2 Program to determine mode cut-off values.**

The following flow-chart (figure 3.1) describes the construction of the program used to calculate the cut-off values for a given waveguide. The main program is called *Cuts m*, and the program which evaluates the cut-off condition at a particular  $U$ ,  $l$  and  $C$  is called *Cutoff m*. The cut-off condition in matrix form is given previously in equation 2.4.7. Any value of  $U$  the core mode parameter, which allows the value of the cut-off condition to be zero is considered to be a cut-off value for a particular  $l$  and  $m$  (the mode indices). It can be seen from equation 2.4.7 that the only other parameter in the equation is the  $C (= b/a)$  value. This means that there is only one set of cut-off values for any  $C$ , regardless of the actual dimensions of the waveguide. This set of cut-off values is the output of *Cuts m*, and is saved in matrix form. The code for both of these programs is given in Appendices A and B.

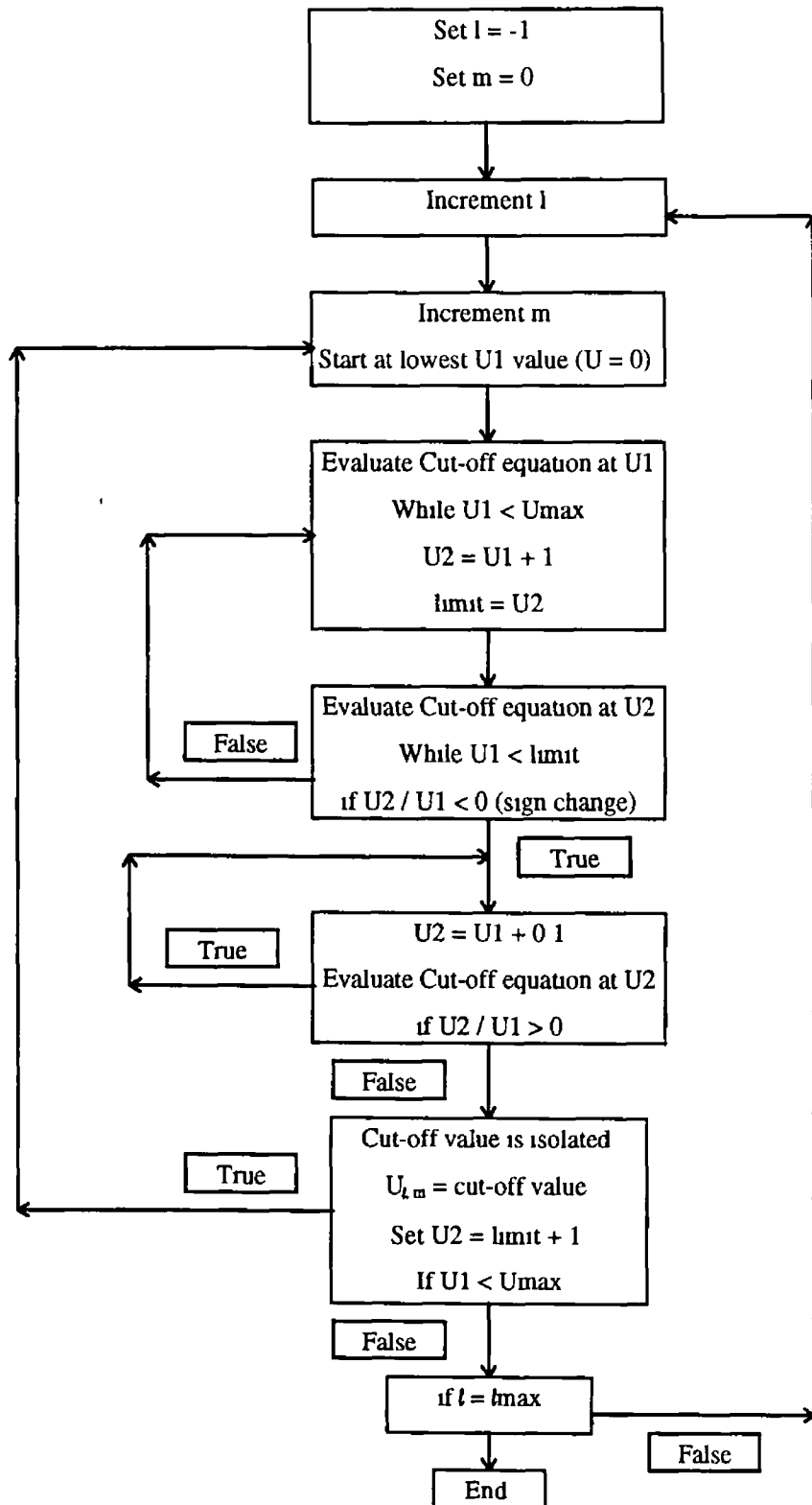


Figure 3-1 Flow chart of program Cuts m

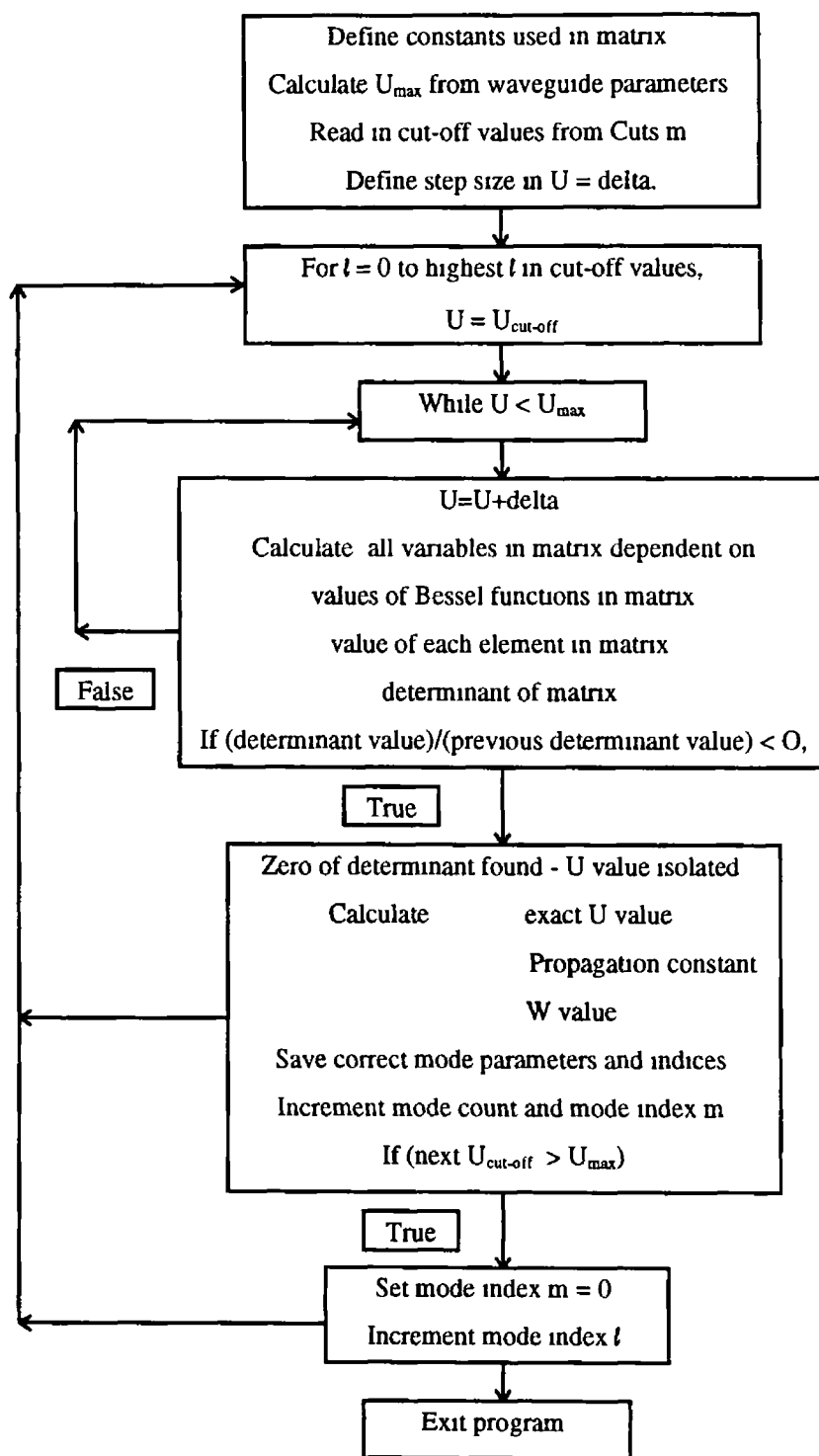


Figure 3-2 Flow chart of Holl m.

### 3.3 Computer program to solve the eigenvalue equation.

This program was called **Holl m**, the code is listed in Appendix C. The purpose of this program is to calculate the allowed U values in the hollow cylindrical waveguide based on the variable parameters entered by the user. To this, the six eigenvalue equations of equations 2.3.1 to 2.3.6 were placed in a matrix form. The determinant of the matrix was then calculated. Each value of U (with a particular l and m) for which the determinant of the matrix equalled zero was considered to be a bound mode within the waveguide, provided the U value was greater than the appropriate cut-off value for its' given mode indices (l and m). An incremental substitution method was used to find the correct U values, with the starting U value being the correct cut-off value, so that this condition was fulfilled automatically. The flow-chart in figure 3-2 shows the logic steps used in **Holl m**, the code is given in Appendix C.

### 3.4 Program to derive E and H field component amplitudes in core and cladding.

The program designed to derive the E and H field component amplitudes was called **Holl\_se m**. The code for this program is given in Appendix D. The purpose of the program was to solve the six equations 2.3.1 to 2.3.6 to find A, B, G, D, E and for each mode found by **Holl m**. This was done by setting A = 1, and solving the resultant 5 equations simultaneously to find B, G, D, E and F. In matrix form this is described as

$$\begin{bmatrix} a_2 & a_3 & a_4 & a_5 & a_6 \\ b_2 & b_3 & b_4 & b_5 & b_6 \\ c_2 & c_3 & c_4 & c_5 & c_6 \\ d_2 & d_3 & d_4 & d_5 & d_6 \\ e_2 & e_3 & e_4 & e_5 & e_6 \end{bmatrix} \cdot \begin{bmatrix} B \\ G \\ D \\ E \\ F \end{bmatrix} = \begin{bmatrix} -a_1 \\ -b_1 \\ -c_1 \\ -d_1 \\ -e_1 \end{bmatrix} \quad \text{Eqn 3.4.1}$$

or in vector notation

$$M\bar{x} = \bar{y}$$

$$\bar{x} = M^{-1}\bar{y}$$

Eqn 3 4 2

Thus the five amplitudes B, G, D, E and F are obtained from the vector  $\bar{x}$  in equation 3 4 2. For each (l, m) mode for which a U and W value are known, the above operation is used to determine the wave amplitudes in the core and in the two cladding regions. The flow-chart to describe the steps in the program **Holl\_se m** is shown in figure 3-3. [Any of the six amplitudes could be set at a fixed value, the choice of A = 1 is purely arbitrary]

### **3.5 Program to evaluate mean evanescent power fraction $\bar{f}$ among modes.**

The Matlab program **Hollpow m** was written to calculate the mean evanescent power fraction  $\bar{f}$  among modes. This was done by calculating the power contained in the core and evanescent fields of each individual mode being guided by the hollow cylindrical waveguide, as identified by the method described above, then finding the fractional representation of evanescent power and calculating the mean over all modes in the waveguide. The formulas used to find the evanescent power fraction are given previously in sections 2.9 and 2.10 (equations 2.9.1 and 2.10.1). The flow-chart to describe **Hollpow m** is shown in figures 3-4 and 3-5 and the code is given in Appendix E.



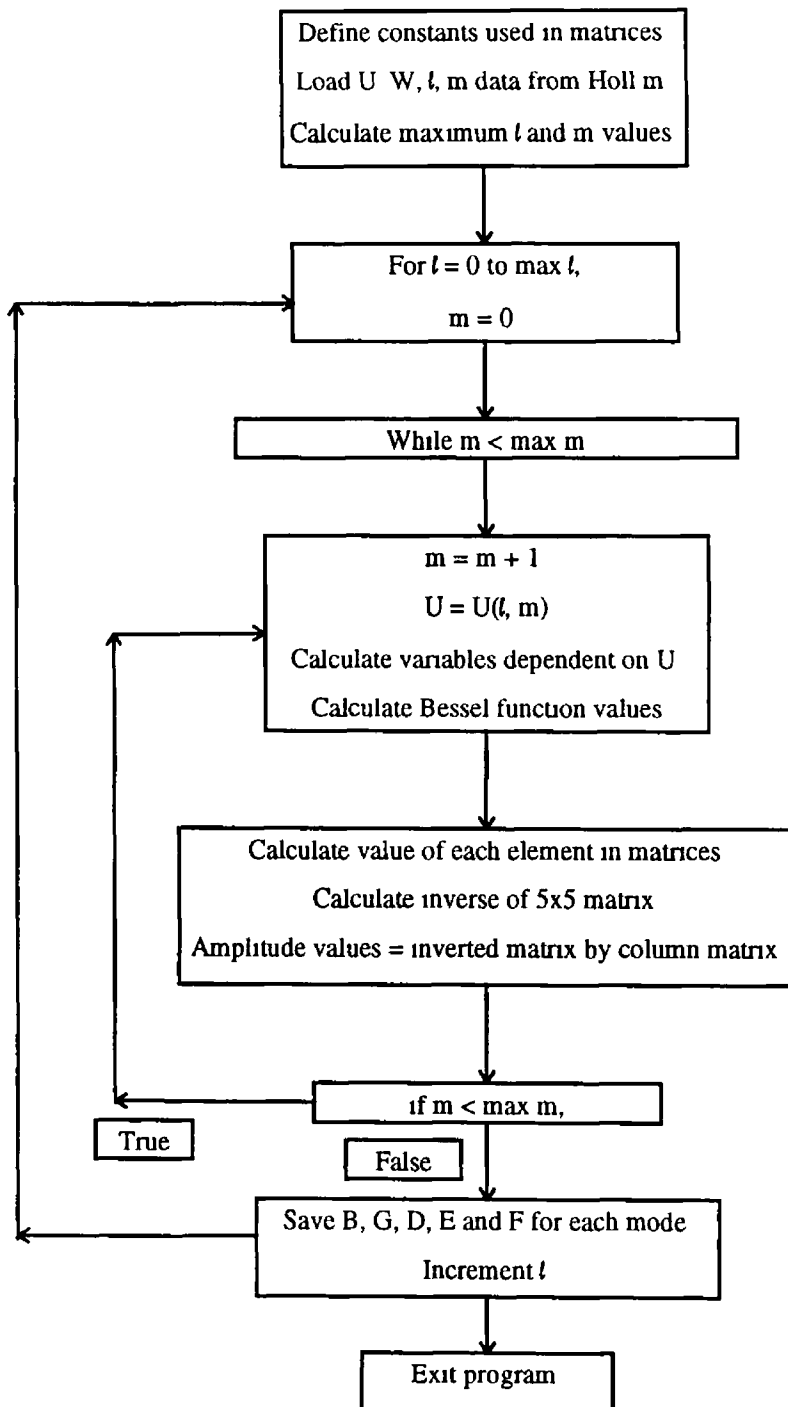


Figure 3-3 Flow-chart for *Holl\_se m*

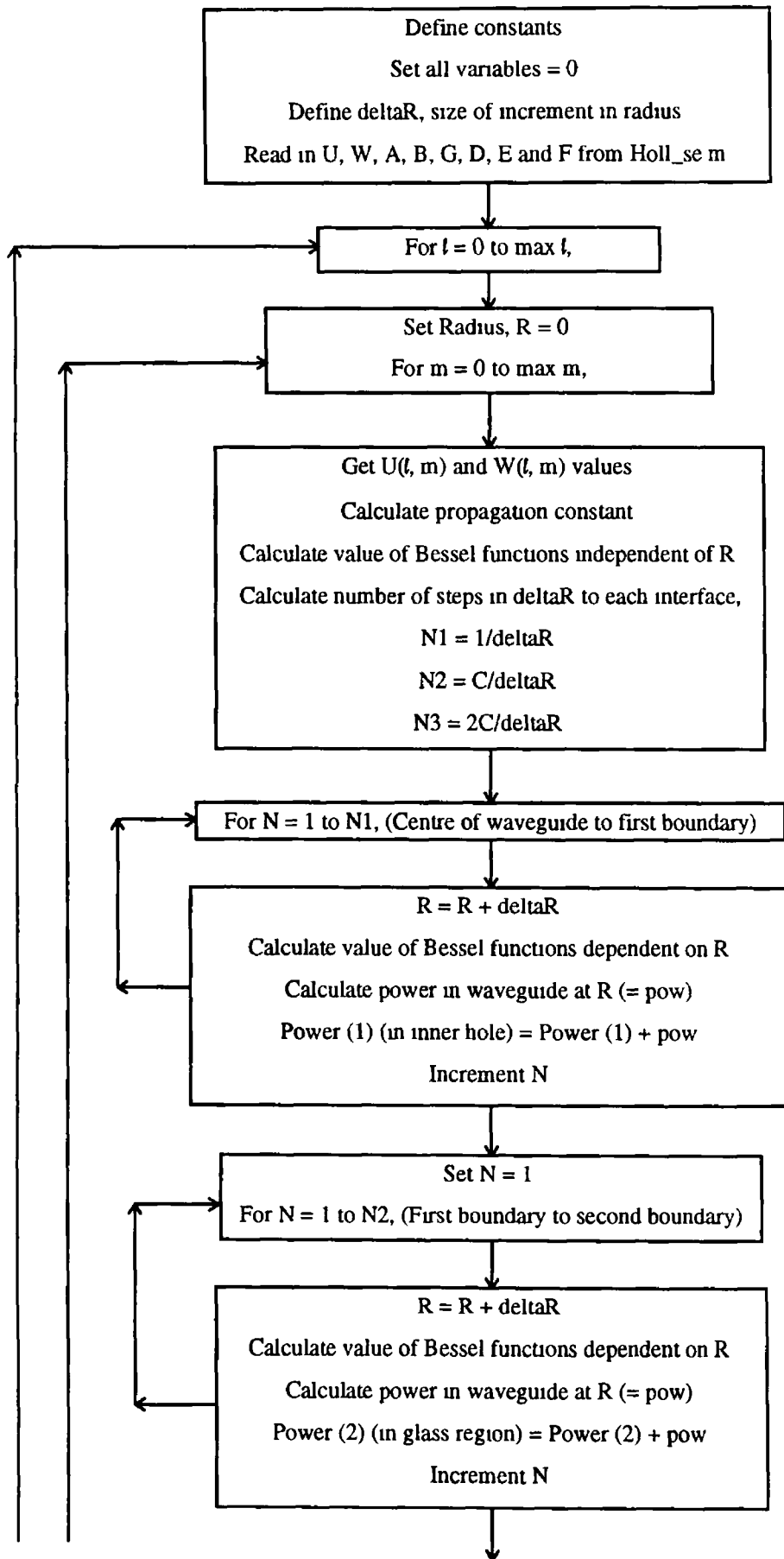


Figure 3-4 Flow-chart for Hollpow m (continued in figure 3 5)

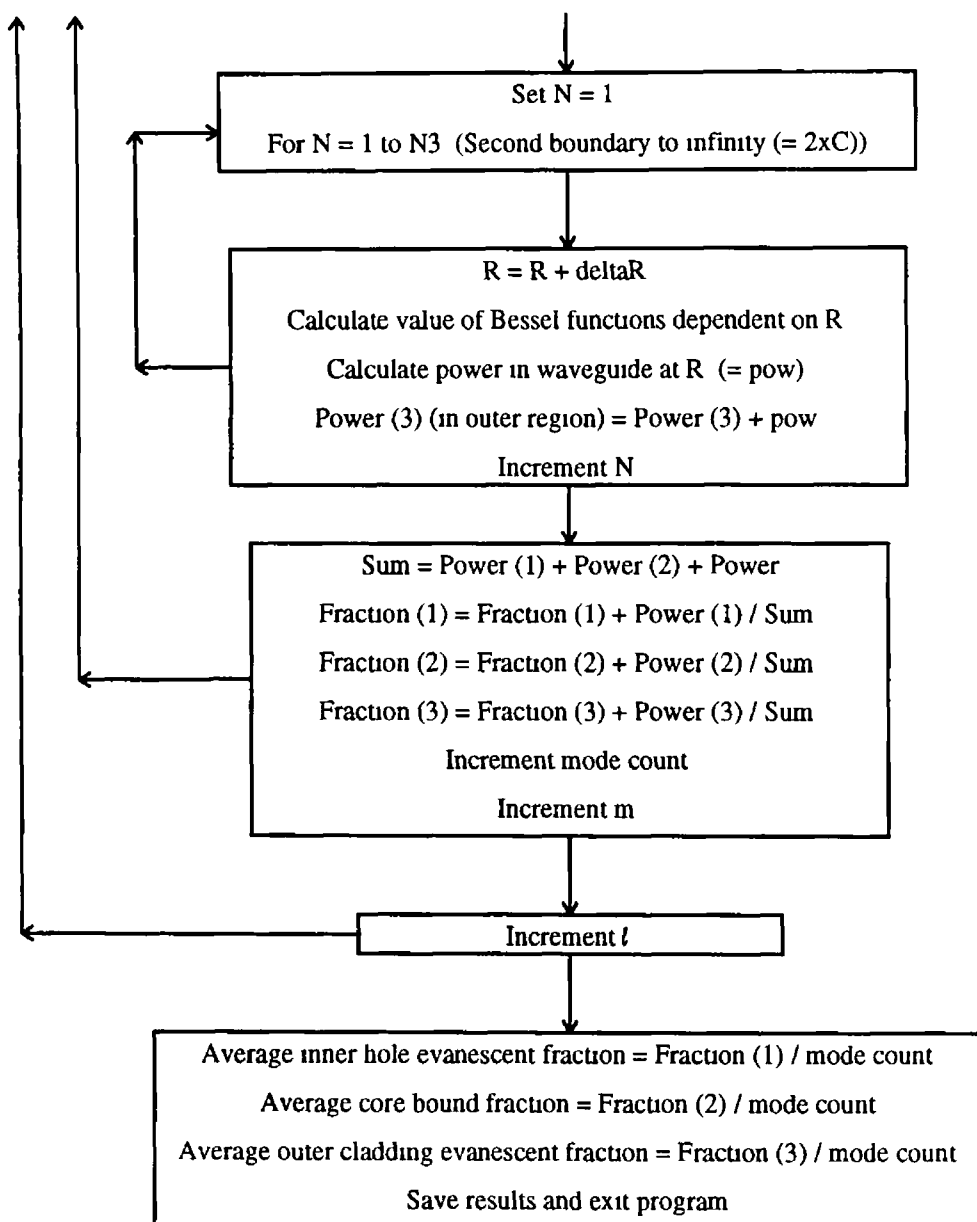


Figure 3-5 Continuation of flow-chart for Hollpow m.

### 3.6 Mode power fraction distribution.

Individual evanescent mode power fractions derived by numerical integration of the Poynting vectors (using **Hollpow m**, and equation 2 10 1) were used to generate a histogram of such fractions and their mean value averaged over all the modes of a particular waveguide. For example, for a waveguide for which  $a = 80\mu\text{m}$ ,  $C = 1.3$ ,  $n_1 = 1.46$ ,  $n_2 = 1.45$  and  $\lambda = 1\mu\text{m}$  (i.e.  $V = 71.226$ ) the modes are predominantly strongly guided with very low evanescent power fractions. The fraction of modes

close to cut-off scales as  $1/V'$  (or 1.4% in this case) It can be seen from table 3-1 that only 0.9% of modes have an evanescent power fraction with a value greater than 0.75 The distribution of modes is shown in figure 3-6

f Value	Percentage of Modes
$f < 0.01$	40%
$f > 0.1$	5 %
$f > 0.5$	2%
$f > 0.75$	0.9%

Table 3-1 f values with corresponding mode percentages

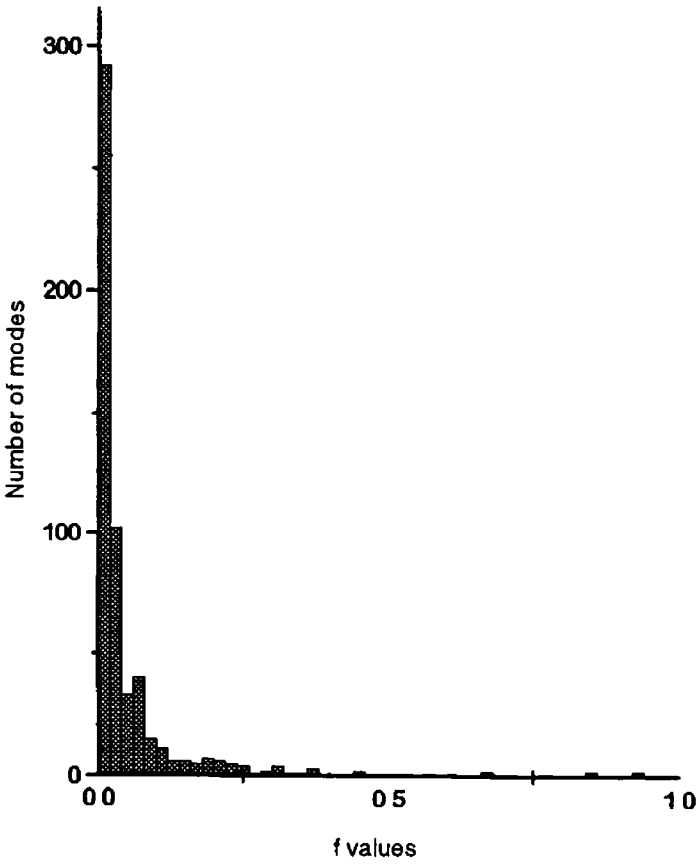


Figure 3-6 Histogram of power fraction  $f$  distribution

### 3.7 Dependence of $\bar{f}$ on $V'$ and $(b/a)$ .

Following the same argument as Gloge (1971) the dependence of the average evanescent power fraction  $f$  on the  $V$  number was investigated. To do this the programs listed above were executed in sequence several times, each time using different inner and outer radii for the dimensions of the hollow waveguide (but the same  $C$  value), while leaving all the other parameters the same (refractive indices and wavelength of transmitted light). This yielded a series of average evanescent power fractions  $\bar{f}$  with corresponding  $V$  numbers. In figures 3-7 and 3-8 the power fractions for the  $C = 1.5$  and  $C = 1.2$  waveguides for  $n_1 = 1.46$ ,  $n_2 = 1.45$ ,  $\lambda = 1\mu\text{m}$  light is plotted against

$$\frac{1}{\sqrt{b^2 - a^2}} \tag{Eqn 3.7.1}$$

to investigate a possible  $1/V'$  dependence.

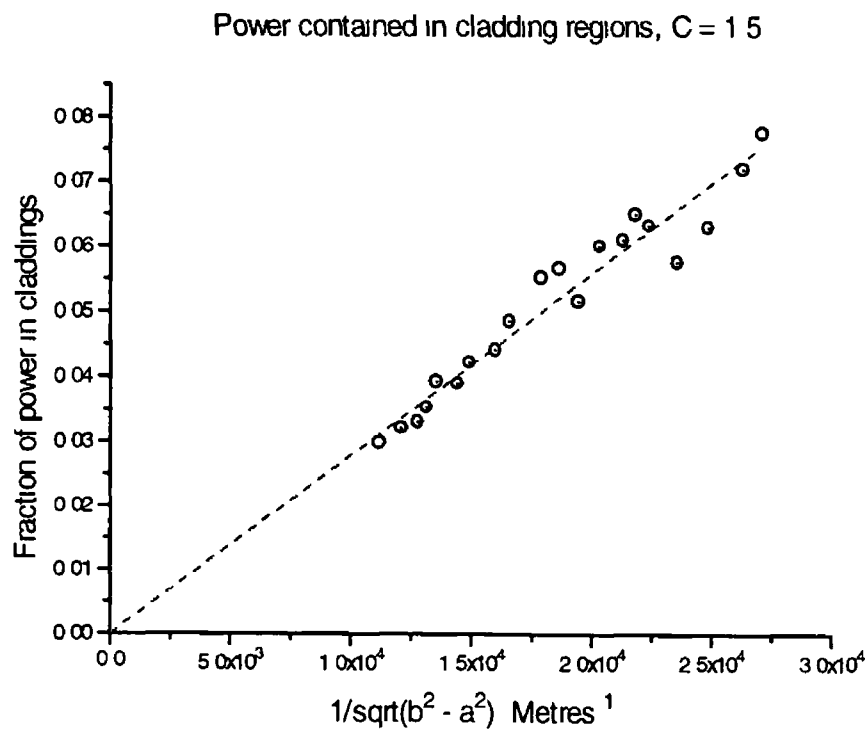


Figure 3-7  $f$  versus  $1/V'$   $C = 1.5$

It can be seen that the numerical model data is scattered about a straight line through the origin, in both cases. The scatter is not unexpected since at a particular  $V'$  number there will be one

mode extremely close to cut-off ( $W = 0$ ) which will give an unusually high evanescent power fraction for that mode

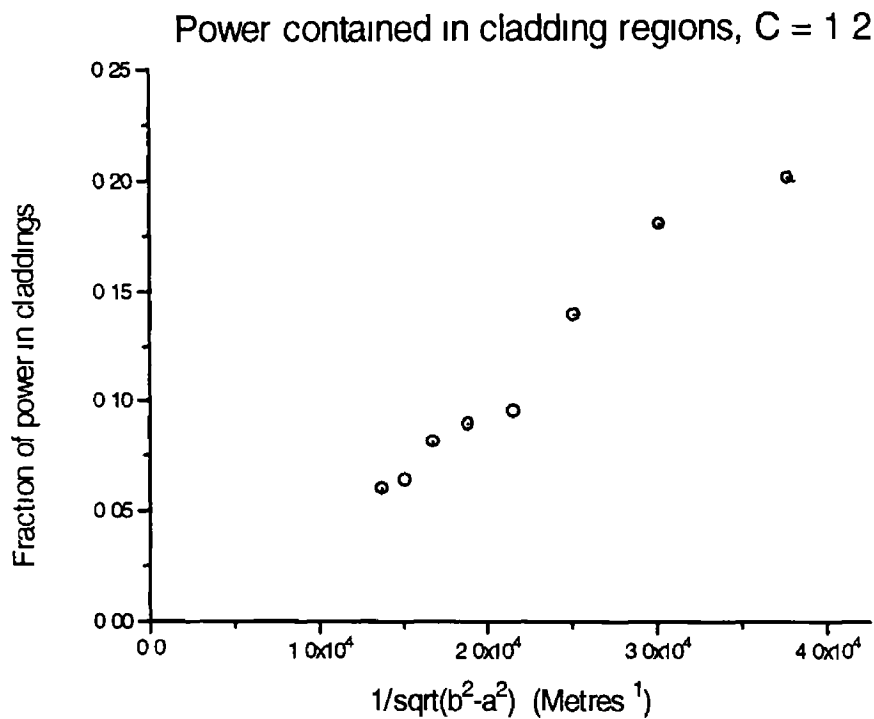


Figure 3.8  $\bar{f}$  versus  $1/V'$   $C = 1.2$

Gloge (1971) has shown that for a step index fibre waveguide the mean evanescent power fraction  $\bar{f}$  averaged over all bound modes is proportional to  $1/V'$  Payne and Hale (1993) find the same dependency with a different multiplicative constant. Both use an approximation in their analysis that  $W \gg l$  for all modes. Numerical modelling of the evanescent fraction in this fibre case without the approximation ( $W \gg l$ ) indicates that

$$\bar{f} \cong \frac{0.8}{V'} \tag{Eqn 3.7.2}$$

By plotting  $\bar{f}$  against  $C$  (figure 3-9) it was found from the data obtained for the hollow cylindrical waveguide model that like the fibre waveguide  $\bar{f}$  scaled linearly with  $1/V'$  with a small dependence on  $C$  given by

$$\bar{f} = \frac{P}{V} \left\{ \frac{C+2P}{C-1} \right\}^{\frac{2}{\pi}} \quad \text{Eqn 3.7.3}$$

where  $P = 0.867$ . In the limit of  $a = 0$  or  $C = \infty$  the effective  $V$  number  $V'$  reduces to the value  $V$  and equation 3.7.2 becomes identical to equation 3.7.3

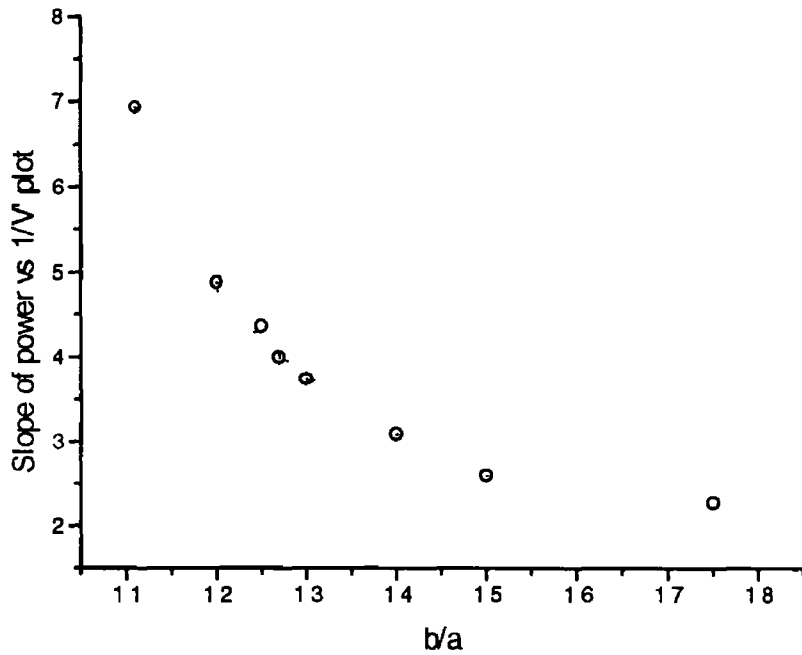


Figure 3-9 Graph of  $\bar{f}$  versus  $C$

### 3.8 Dependence of $N$ on $V'$ .

It has been shown in section 2.6 that the total number of bound waveguide modes is predicted to scale approximately as  $V'^2$  or as  $(b^2 - a^2)'$  ( $V'$  is defined in equation 2.7.2). This was verified numerically by counting modes for various waveguide dimensions, as shown in figures 3-10 and 3-11 with  $C = 1.2$  and  $1.5$  respectively. The mode number values were provided by the **Hollpown** program. A very good fit for the total number of modes versus  $(b^2 - a^2)$  was obtained, verifying the  $N = V'^2/2$  type of relationship for the hollow waveguide.

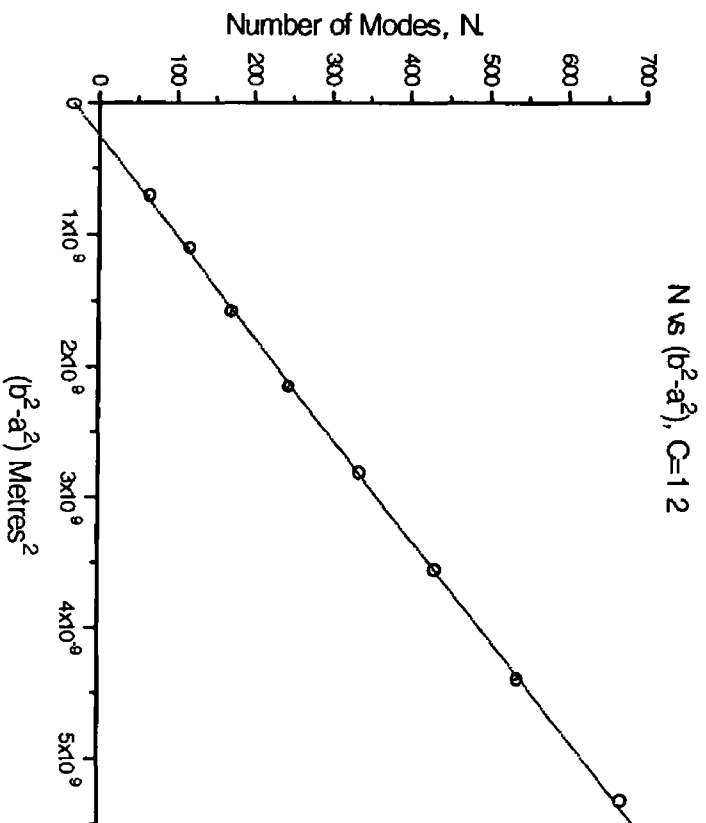


Figure 3-11  $C = 12$



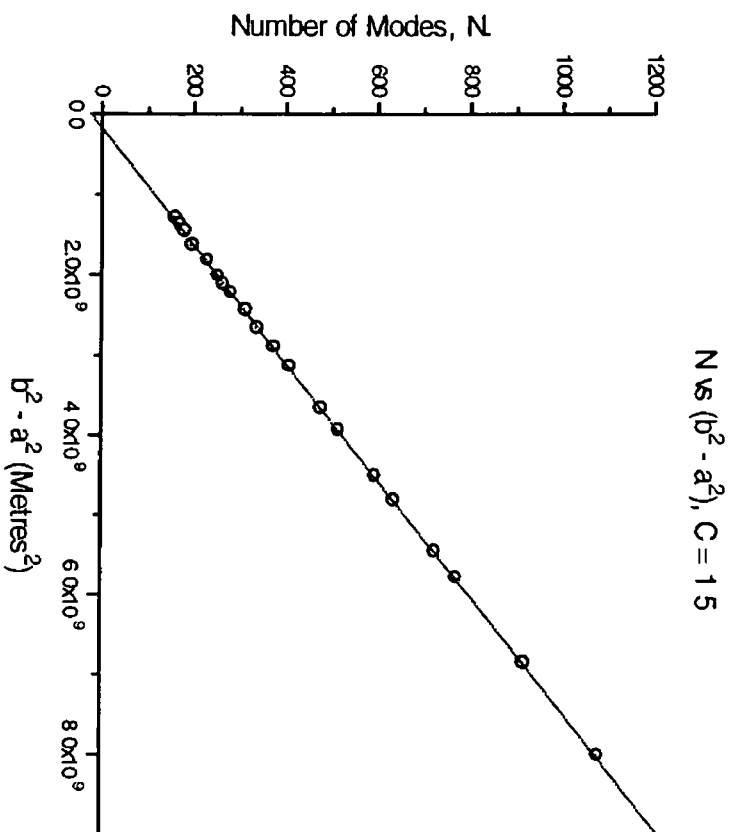


Figure 3-10  $C = 1.5$

### **3.9 Conclusions.**

The computer programs listed above represent a model of the effect a hollow cylindrical waveguide has on light being transmitted through it. The model parameters can be varied in terms of refractive index of the core and cladding, the waveguide dimensions and the wavelength of light being transmitted through it. The model yielded theoretical relationships between the number of modes,  $N$ , the mean evanescent power fraction,  $\bar{f}$ , and the effective  $V$  number,  $V'$ , and showed the interdependence of the various parameters.

### ***3.10 References.***

Gloge D, "Weakly Guiding Fibers", Appl Opt 10 pp 2252 - 2258 (1971)

Payne F P and Hale Z M, "Deviation from Beer's Law in Multimode Optical Fiber Evanescent Field Sensors", Int J Optoelectronics, 8 (5/6) 743 - 748 (1993)

## **4. Evanescent wave spectrophotometry using a hollow waveguide probe.**

### **4.1 Introduction.**

The design of an Attenuated Total Reflectance (ATR) Hollow Cylindrical Sensing probe and an absorbance detection system is described. Uniform mode excitation is achieved using a series of launch step-index fibers butt coupled to the ATR probe.

### **4.2 The ATR probe.**

A length of fused silica hollow tubing of inner diameter (2a) 9.32 mm and outer diameter (2b) 11.863 mm was chosen as the sensor probe. The rod was cut to a length of 280 mm, using a diamond saw and polished at both ends on a Logitech PM2A Lapping Machine, with a set of water based grits of decreasing diameter from 10  $\mu\text{m}$  to 1  $\mu\text{m}$ . For the polishing the silica was supported in a stainless steel disk, and kept vertical by strapping to the central shank of the "polishing tree". Regular inspection of the end (i.e. cut) surfaces was carried out to ensure that all surface blemishes were removed by the coarse grit lapping and polished to a high transparency by the final fine grit.

### **4.3 Excitation of modes in the probe.**

As discussed briefly in section 4.1 excitation of the modes in the hollow waveguide was achieved by butt coupling an array of step index fibers (CeramOptec GmbH OPTRAN H-UV 1000/1035) to one end of the probe. This was done using a machined aluminum plug to which the fibers were epoxied as shown in figure 4-1. The plug was lodged into the waveguide using an o-ring seal.

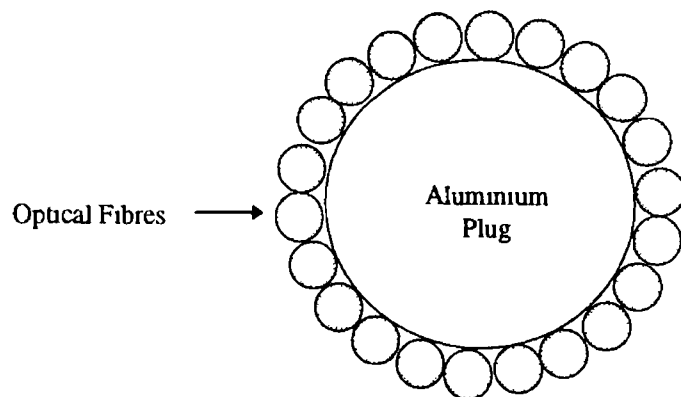
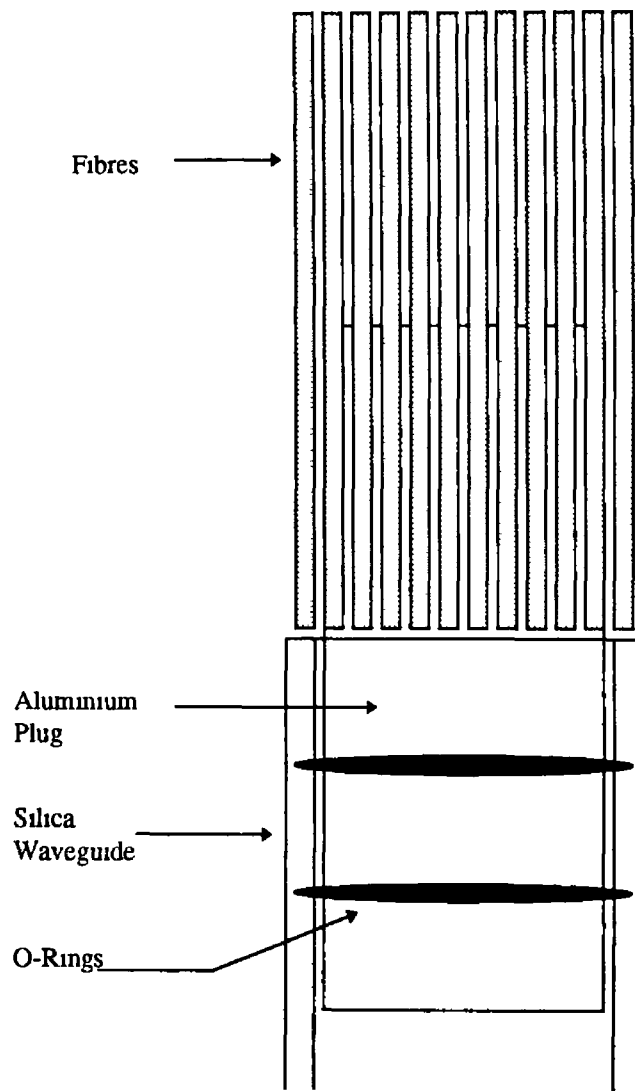


Figure 4-1 Aluminum plug with fibers attached

Light from a 20 W Tungsten halogen light source, powered by a 6 V dc supply was focussed by a 50 mm diameter 65 mm focal length convex-concave lens combination (convex effect) into the fiber bundle as shown in figure 4-2 below. To provide stable emittance conditions the lamp was run below its' 3.3 A rating, a figure of 2.5 A was found to be sufficient. With no liquid surrounding the probe a bright ring of light was observed at the other end of the probe indicating a uniform excitation of the modes in the waveguide probe.

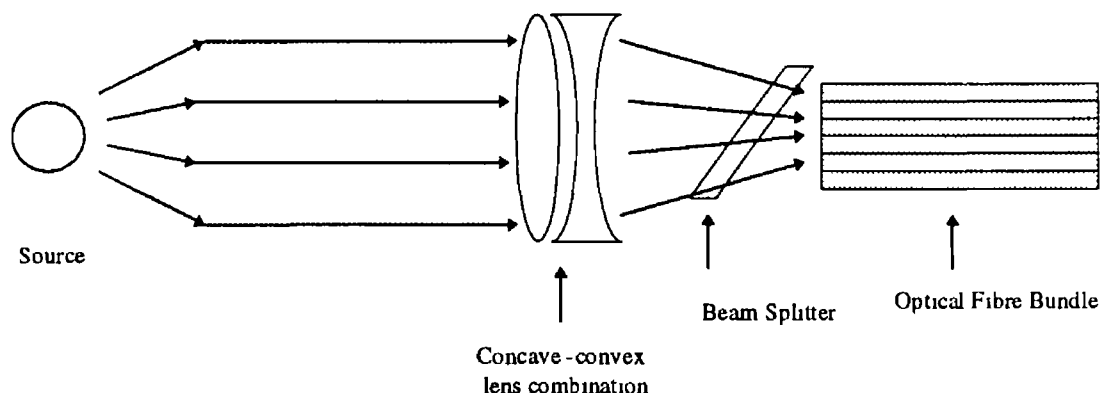


Figure 4-2 Light being focussed into fiber bundle

#### 4.4 Theoretical absorbance of hollow waveguide probe.

The probe dimensions listed in 4.1 lead to a value of the dimensionless constant  $C (= b/a)$  of 1.2728 from the average values of a series of measurements of  $a$  and  $b$ . The refractive index  $n_1$  of fused silica was taken as 1.46. In order to determine the effective  $V$  number of the waveguide its' numerical aperture  $NA$  must be determined, i.e.  $NA = (n_1^2 - n_2^2)^{1/2}$ . The solution used for evaluation of the probe was Eosin Yellow ( $C_{20}H_6Br_4Na_2O_5$ ) in Methanol. Eosin yellow has an absorption band centred at 524 nm. At the concentrations used the refractive index of the solutions were that of Methanol namely 1.3276. Taking  $n_1 = 1.46$ ,  $n_2 = 1.3276$  gives a probe numerical aperture of 0.607. Because this numerical aperture is quite large and because the probe was to be excited by light from a set of step index fibers (of small numerical aperture) butt coupled to one end, the limiting numerical aperture of the system was the smaller of the two, which in this case was the  $NA$  of the fibers. This excitation using fibers will be discussed in a subsequent section. Here the value of  $(n_1^2 - n_2^2)^{1/2}$  will be

taken as the numerical aperture of the fibers, namely 0.37. Using equation 2.7.2 with  $\lambda = 524$  nm the effective V number of the hollow tube waveguide is then 16281.214. Using equation 3.7.3 the theoretical mean evanescent power fraction  $\bar{f}$  is then  $245.389 \times 10^{-6}$  (where P is set at 0.867 and C at 1.2728).

It has been shown in section 1.6 that for an individual mode the transmitted intensity is related to the launched intensity ( $I_0$ ) by

$$I = I_0 \exp(-\alpha f z) \quad \text{Eqn 4.4.1}$$

If all N modes are excited with equal incident power ( $I_0/N$ ) then the transmitted power (after a length z of absorbing region) is

$$I = \sum_{n=1}^N \frac{I_0}{N} \exp(-\alpha f_n z) \quad \text{Eqn 4.4.2}$$

so that the absorbance  $A' = \log_{10} (I_0 / I)$  is given by

$$A' = -\log_{10} \left\{ \frac{\sum_{n=1}^N \exp(-\alpha f_n z)}{N} \right\} \quad \text{Eqn 4.4.3}$$

When  $\alpha f z \ll 1$  for all modes equation 4.4.3 can be evaluated using the expansion  $\exp(-x) \cong 1 - x$  in which case

$$\begin{aligned} A' &= -0.434 \log_e \left\{ \frac{\sum_{n=1}^N 1 - \alpha f_n z}{N} \right\} \\ &= -0.434 \log_e \left\{ 1 - \alpha z \frac{\sum f_n}{N} \right\} \\ &= -0.434 \log_e (1 - \alpha z \bar{f}) \end{aligned} \quad \text{Eqn 4.4.4}$$

where  $\bar{f}$  is the mean evanescent power fraction. Using the expansion  $\log(1-x) \cong -x$  for small x therefore gives

$$A' = 0.434\alpha z\bar{f} \quad \text{provided } \bar{f}\alpha z \ll 1 \quad \text{Eqn 4.4.5}$$

i.e. absorbance scales linearly with  $\bar{f}\alpha z$

When  $\alpha z \bar{f} \gg 1$  the absorbance of equation 4.4.3 is more complicated and leads to a saturation of absorbance with increasing  $\alpha$ , or increasing  $z$ , or increasing  $\alpha z$

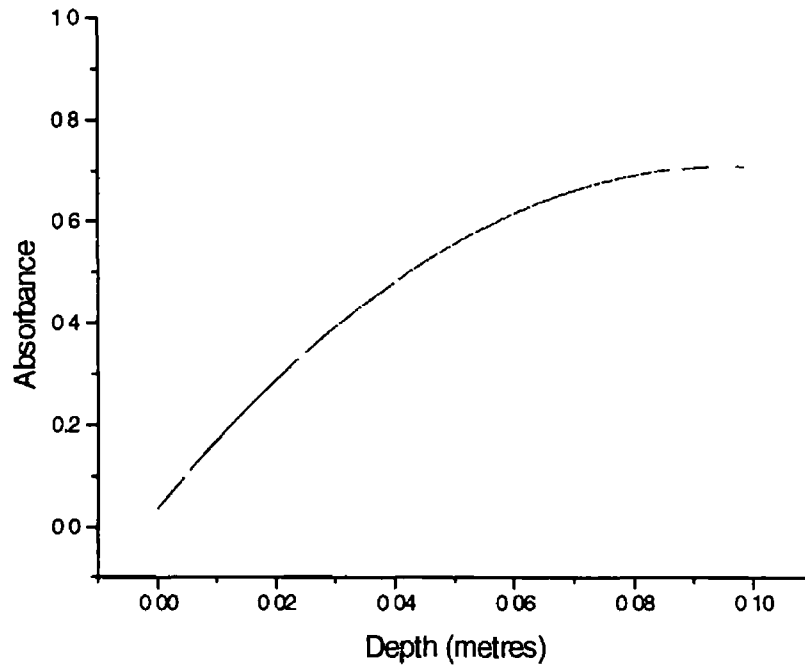


Figure 4-3 Example of saturation of absorbance with increasing depth

#### 4.5 Absorbance measurement technique.

As shown in figure 4-2 light was launched into the probe using a beam splitter. A small fraction of this light is back reflected at the distal end where the probe's annular tip interfaces with the liquid. Because the numerical aperture of the probe is quite small, modes strike the end face at angles very close to the normal and are reflected with a power reflection coefficient of approximately

$$R = \left[ \frac{n_1 - n_2}{n_1 + n_2} \right]^2 \quad \text{Eqn 4.5.1}$$



(the Fresnel reflection coefficient for normal incidence) [It is shown in Appendix G that for a practical range of incident angles  $\theta_i$  the reflection coefficient  $R$  is approximately independent of  $\theta_i$ ]

If an intensity  $I_0$  is launched into the probe (at a wavelength  $\lambda$ ) then  $I_0 \exp(-\bar{f}\alpha z)$  reaches the endface,  $R_0 I_0 \exp(-\bar{f}\alpha z)$  is reflected and  $R_0 I_0 \exp(-2\bar{f}\alpha z)$  is returned to the launch fibers. This is based on absorption occurring at an analytical wavelength. At a wavelength well removed from the absorption band - the so-called reference wavelength - a back reflected intensity of  $R I_0$  occurs (i.e. no attenuation). Thus an evanescent power absorbance ( $A'$ ) of

$$A' = \log_{10} \left\{ \frac{R I_0}{R I_0 \exp(-2\bar{f}\alpha z)} \right\} \quad \text{Eqn 4.5.2}$$

$$= (0.434)(2\bar{f}\alpha z), \quad \bar{f}\alpha z \ll 1$$

is obtained. This is the previously derived expression of equation 4.4.5 but doubled for 2 way travel of the evanescent wave along the probe length  $z$ . As before equation 4.5.2 applies provided  $\bar{f}\alpha z \ll 1$ . As previously defined  $\alpha$  is the bulk attenuation coefficient of the absorber and  $z$  is the immersion depth of the probe in the absorber. By comparing the back-reflected light intensity at the analytical and reference wavelength then the absorbance of the probe can be measured.

Two interference filters were used to isolate a wavelength band centered at  $\lambda = 525 \text{ nm}$  (where Eosin Yellow has an absorption band) and  $\lambda = 430 \text{ nm}$  in the blue to one side of the absorption band. The filters were supported on a mechanical slide and could be placed in turn in front of the entrance window of a Hamamatsu 931A photomultiplier tube. The photomultiplier was operated in the "grounded anode" mode, the detector signal being extracted as a voltage across a  $10 \text{ M}\Omega$  resistor. The light entering the launch fibers was modulated using a mechanical chopper which operated at a chopping frequency of  $330 \text{ Hz}$ . The chopper drive unit (Scitex Instruments optical chopper) supplied the square wave pulse train to synchronise phase sensitive detection with a lock-in amplifier. The PM output was fed by coaxial cable to the signal input of an EG&G model lock-in amplifier (model 950VG) whose post filter time constant was set at 3 seconds.

An absorbance measurement then involved recording two output voltages from the lock-in amplifier corresponding to each optical filter being in the light beam returning to the photomultiplier.

detector. A series of back reflected intensity measurements, with the probe enclosed in a light tight box, was made to determine if any drift occurred in either (i) the light source intensity or (ii) the photomultiplier output. It was found that the lamp intensity stabilised in 45 minutes after switching on, and there was no detectable photomultiplier drift over a 2 hour period. The PM was powered by a 500 V EHT unit (EMI electron tube division Power Supply PM28B).

#### **4.6 Conclusions.**

A relatively simple back-reflection ATR probe, excited by light from a tungsten halogen lamp via an array of step index fibers butt coupled to one end and operated in phase sensitive detection, was constructed. The evanescent light in both the inner hole and surrounding medium may be used to analyse fluids with absorption bands in the visible using a dip-stick style of approach. All optics are concentrated at one end of the probe.

## 5. Experimental absorbances using hollow silica waveguide.

### 5.1 Introduction.

Absorbance measurements made with the ATR analyser probe discussed in chapter 4 are reported here. Results are compared to the mode model predictions of chapters 2 and 3.

### 5.2 Bulk properties of the absorbing cladding.

As stated earlier a solution of Eosin Yellow in Methanol was chosen as the absorbing cladding with which the hollow cylindrical ATR probe was to be evaluated. The bulk absorption properties of this chemical at  $\lambda = 524$  nm were examined using a SHIMADZU (UV - 1201) UV-VIS spectrophotometer. Solutions of various molar concentrations ( $1M = 0.69186$  gram/cc of solute) were prepared and their bulk absorbances (at 524 nm) were measured. In each case a cuvette containing the solution was inserted in the spectrophotometer beam and the beam attenuation compared to that of the solute (methanol) on its own. A graph of absorbance versus solution concentration (figure 5-1) was prepared and a least-square fit line generated through the data points (using an "Origin" subroutine). From the best-fit slope the bulk absorption coefficient  $\alpha$  for Eosin Yellow was found. For a 1M solution  $\alpha$  was found to be  $\alpha = 23250.0 \text{ mm}^{-1}$  (or  $0.02325 \text{ mm}^{-1} \mu\text{M}^{-1}$ ).

For a weaker solution - say of concentration  $10^{-3} \text{ M}$ , the corresponding  $\alpha$  value is 1000 times smaller. For evanescent wave absorption the parameter of interest is  $\bar{f}\alpha$ , where  $\bar{f}$  is the mean evanescent power fraction among the modes.

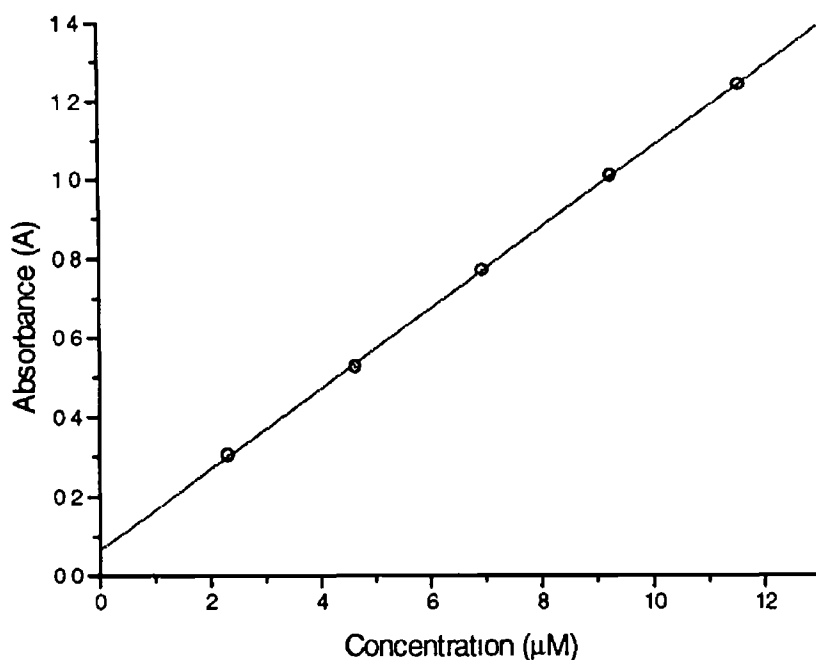


*Figure 5-1 Bulk absorbance versus solution concentration*

### **5.3 Evanescent absorbance as a function of probe immersion depth.**

We have seen in section 4.4 that the evanescent absorbance  $A'$  is predicted to scale linearly with the product  $\bar{\rho} \omega z$ . For a probe of constant dimensions ( $a$ ,  $b$ ) the evanescent absorbance is predicted, therefore, to scale linearly with the immersion depth  $z$ . This was investigated experimentally.

A solution of 28.756  $\mu\text{M}$  Eosin Yellow in Methanol was prepared and placed in a graduated cylinder which could be raised or lowered around the hollow ATR probe. A series of absorbance measurements (at  $\lambda = 524 \text{ nm}$ ) were made as a function of the immersion depth  $z$ . These results are shown in figure 5-2.

The functional relationship of equation 4.4.2 is vindicated in this straight line graph. The saturation effect alluded to in section 4.5 for high concentrations of solution or large immersion depths (i.e. when  $\bar{f}oz \geq 1$ ) was observed with this probe.

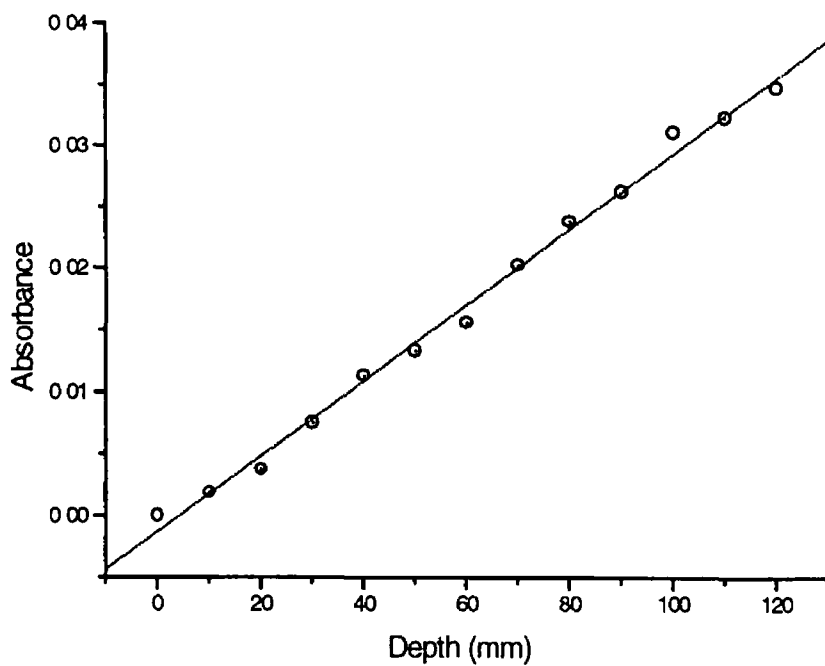


*Figure 5.2 Evanescent absorbance versus depth (28.756  $\mu$ M solution)*

A 306.902  $\mu$ M solution was used with the same immersion depth. Results are shown in figure 5-3.

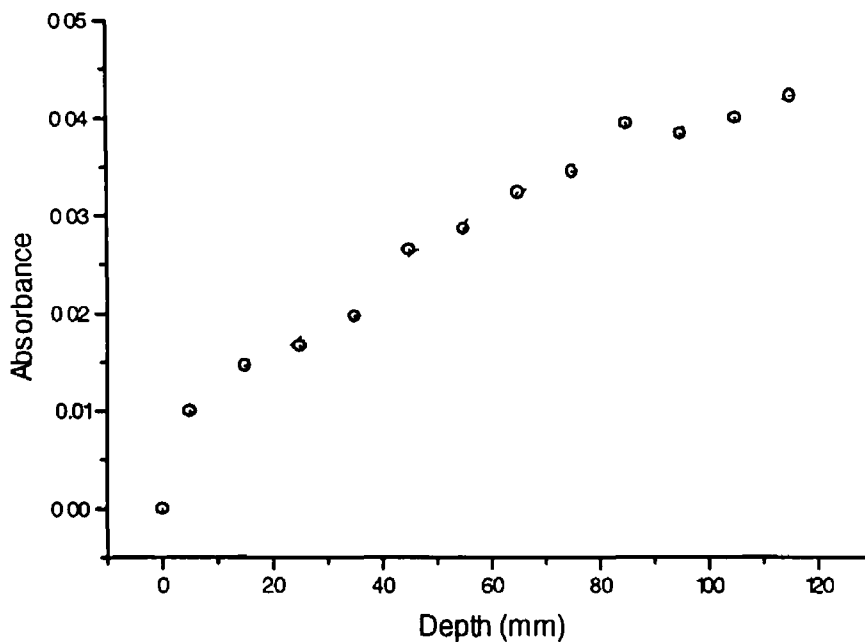


Figure 5-3 Evanescent absorbance versus depth, 306.902  $\mu\text{M}$  concentration

It can be seen that the complete absorption of some modes or the differential attenuation of the modes - varying from weak attenuation for modes far from cut-off ( $U \ll V$ ) to strong attenuation for modes near cut-off ( $U \approx V$ ) - gives rise to a non-linear dependence of absorbance on immersion depth ( $z$ ), for fixed concentrations. This effect was predicted in section 4.3. This effect also occurs in solid cylindrical fibre evanescent wave probes as observed by Ruddy (1994). In the intervening region, i.e. of concentration from 28  $\mu\text{M}$  to 306  $\mu\text{M}$  a family of absorbance versus immersion depth curves were obtained at various concentrations. These showed a gradual transition from linearity (for low concentrations of  $\sim 30 \mu\text{M}$ ) to saturation for higher concentrations.

#### 5.4 The experimental $\bar{f}$ value.

For the weak solution ( $\bar{f}\alpha z < 1$ ) the linear absorbance graph of figure 5-2 can be used to extract an experimental  $\bar{f}$  value. The graph slope ( $s$ ) of 0.0003 combined with a bulk absorption coefficient  $\alpha$  of 0.668577  $\text{mm}^{-1}$  (for 28.756  $\mu\text{M}$  Eosin Yellow solution) yields an experimental  $\bar{f}$

value of  $224\,3571 \times 10^{-6}$ . This may be compared to the theoretical value of equation 3.7.3 taking  $P = 0.867$ ,  $C = 1.2728$ ,  $V' = 16281.214$  of  $\bar{f} = 245\,38957 \times 10^{-6}$ . This is a difference of 8.57%. It can be seen that the mode modelling of chapters 2 and 3 and the experimental measurement of chapter 5 are in very good agreement.

## 5.5 Conclusions.

Experimental measurements of absorbance using a hollow cylindrical ATR probe were used to extract a mean evanescent power fraction ( $\bar{f}$ ) among all the bound modes of the waveguide. Good correlation between the experimentally derived  $\bar{f}$  values and that predicted by rigorous mode analysis for such a waveguide indicates the latter. It should be stated that the mode analysis carried out does not assume the “weakly guiding” approximation ( $n_1 \cong n_2$ ) as in general with glass based probes and liquid absorber solutions that approximation (commonly used in step-index fibre mode analysis) is not valid.

## ***5.6 References.***

Ruddy V, "Non linearity of absorbance with sample concentration and path length in evanescent wave spectroscopy using optical fibre sensors", Optical Engineering 33, no 12, pp (3891-2893) (1994)



# Appendix A

The following is the Matlab code for the **Cuts m** program. Any lines starting with a '%' sign are comments on the code, not part of the code itself, and are ignored by the Matlab compiler.

```
% Title  Cuts m

% Aim  To calculate cut off values for a hollow cylindrical waveguide by stepping through the cut
% off equation until the zeros are located

delta_x = 1,          % step size in U

x1 = 1,               % starting value for U

for j = 0:j_max,      % loop through all orders, where j is the order l

    count = 1,        % resets the count of U values in each l order

    y1 = cutout(j,x1,C), % calculate value of cut-off equation

    while (x1 < x_max), % step through all U values

        x2 = x1 + delta_x, % increment U by delta U

        limit = x2,        % stores largest U value tested so far

        y2 = cutout(j,x2,C), % calculate value of cut-off equation

        test = x1,         % stores next largest U value tested so far

        if ((y2/y1) < 0), % if sign change occurs, root is isolated

            while (test < limit),

                x2 = x1 + (delta_x/10), % increase U value by 10% of delta U

                y2 = cutout(j, x2, C) % calculate value of cut-off equation

                if (y2/y1) > 0, % if sign change has not occurred
```

```

        x1 = x2 + delta_x/10,    % increase U value by 10% of
                                % delta U

        y1 = cutout(j,x1,C),    % calculate value of cut-off
                                % equation

    else

        slope = (y2 - y1)/(x2 - x1), % sign change has occurred

        U = x1 - (y1/slope),      % calculate correct root value

        ucut(j+1,count) = U,      % save U value in array

        count = count + 1,        % increment counter

        test = limit+1,          % make 'test' > 'limit'

    end,                          % end of 'if(y2/y1) > 0' statement

    y1 = y2,                    % prepare for next run through loop

    x1 = x2,                    % prepare for next run through loop

end,

else

    y1 = y2,                    % prepare for next run through loop

    x1 = x2,                    % prepare for next run through loop

end,                          % end of 'while (test < limit),' statement

end,                          % end of 'if (y2/y1) < 0)' statement

if count == 1,                % if no cutoffs are found

    break,                    % exit 'while (x1 < x_max),' loop

end,

if j > 0,

```

```

        if ucut(j,1) < x_max,      % if all roots of present order  $l$  have not yet been found,

            x1 = ucut(j+1,1), % start searching at last known U value

        end,

    else

        x1 = 6,      % reset to lowest U value, to search next  $l$  order

    end,

    ucut(j, )      % output to screen all found U values

end,    % end of 'j = 0 j_max' loop

```

## Appendix B

This program evaluates the cut-off equation at values passed to it from the program that called it in this case the calling program is Cuts m

```
% Title  Cutout m
```

```
% Aim  To calculate value of cut off equation at a given U value
```

```
function[y_val] = cutout(j,x,C)    % defines the function name and the number and value of  
variables                          % the function will use
```

```
y1 = (besselj(j,x) * bessely(j,C*x)),    % defines the equation parts used in the function
```

```
y2 = (besselj(j,C*x) * bessely(j,x)),
```

```
y_val = y1 - y2,    % calculates the value of the function at the specified parameter values,
```

```
% and returns this value to the calling program
```

## Appendix C

This program finds the correct U values for each order by using the cut-off values calculated by

Cuts m

% Program title holl8 m

% Purpose To establish the correct modes for each order of  $H$  function in a hollow cylindrical

% waveguide

% Method To cycle through a range of U values and calculate the determinant of the matrix for each

% value until all the values for which the determinant is zero are found

global i, % declares 'i' as a variable used throughout the program

$k = (2 * \pi) / \lambda$ , % calculates the wavenumber k

$Z = 377$ , % defines the characteristic impedance of free space

$j = 1$ ,

$p = -k * Z$ , % substitutional variable

$q = k / Z$ , % substitutional variable

$\beta(1) = n_1 * k$ , % sets the value of the propagation constant

$U_{\max} = n_{\text{rad}} * \sqrt{(n_1^2 * k^2) - (n_2^2 * k^2)}$ , % calculates the maximum U value

$\delta = 0.01$ , % sets the step size in U

$\text{limit} = (U_{\max} * 100) - \delta$ , % calculates the limit in steps of delta

$u(1) = 0.0$ , % sets starting U = 0

$t = 1$ ,

```

fid = fopen('holl8a.tmp','w');           % opens a file for output.

for i = 1:length(ucut),                   % length(ucut) is the size of the array holding cut-off values.

    if ucut(i,1) > U_max,                  % if first value of any row (i) is > U_max.

        j_lim = i-2;                      % sets limit of 'j' loop.

        break;                            % break out of loop.

    end;                                  % end of 'if' statement.

end;                                      % end of 'for' loop.


x = 0;                                    % initialise x variable.

for j = 0:j_lim;                          % for every order (j) from 0 to j_lim in steps of 1.

    x = x+1;                              % increment x.

    i = 3;

    t = 1;

    while i < limit,                      % limit is defined at U_max - delta.

        % u(i) is incremented from cut off value

        % there is no zeroth row in array, so order 0 values stored in 1st row.

        u(i) = ucut(j+1,x) + (t*delta);    % u set at cut-off value + (t*delta),

        t = t+1;                          % counter of number of increments on u.

        beta(i) = sqrt((n1^2*k^2) - (u(i)^2/in_rad^2)); % calculate propagation const.

        U = u(i);                          % set value of core mode parameter.

        W = in_rad * sqrt(beta(i)^2 - (n2^2*k^2)); % calculate cladding mode parameter.

        UC = out_rad * sqrt((n1^2*k^2) - beta(i)^2); % calculate U*C.

```

WC = out\_rad \* sqrt(beta(i)^2 - (n2^2\*k^2)), % calculate W\*C

BJU = besselj(j,U), % calculate value of Bessel J at U

DBJU = -besselj(j+1,U) + (j/U)\*BJU, % calculate value of Bessel J derivative

BJUC = besselj(j,UC), % calculate value of Bessel J at UC

DBJUC = -besselj(j+1,UC) + (j/UC)\*BJUC, % calculate value of Bessel J derivative

BYU = bessely(j,U), % calculate value of Bessel Y at U

DBYU = -bessely(j+1,U) + (j/U)\*BYU, %calculate value of Bessel Y derivative

BYUC = bessely(j,UC), % calculate value of Bessel Y at UC

DBYUC = -bessely(j+1,UC) + (j/UC)\*BYUC, % calculate value of Bessel Y  
% derivative

BIW = besselj(j,W), % calculate value of Bessel I at W

DBIW = besselj(j+1,W) + (j/W)\*BIW , %calculate value of Bessel I derivative

BKWC = besselk(j,WC), % calculate value of Bessel I at WC

DBKWC = -besselk(j+1,WC) + (j/WC)\*BKWC, % calculate value of Bessel I  
% derivative

BKW = besselk(j,W), % calculate value of Bessel K at W

$DBKW = -\text{besselk}(j+1, W) + (j/W) * BKW$ , %calculate value of Bessel K derivative

% x1-4 and y1-6 are substitutional variables used in the matrix

$$x1 = BJUC / BJU,$$

$$x2 = BYUC / BYU,$$

$$x3 = BKWC / BKW,$$

$$x4 = (1/U^2) + (1/W^2),$$

$$y1 = DBIW / BIW,$$

$$y2 = DBJU / BJU,$$

$$y3 = DBYU / BYU,$$

$$y4 = DBYUC / BYU,$$

$$y5 = DBKWC / BKW,$$

$$y6 = DBJUC / BJU,$$

% the following are the elements of the 6\*6 matrix,

$$a1 = x1,$$

$$a2 = x2,$$

$$a3 = 0,$$

$$a4 = 0,$$

$$a5 = -x3,$$

$$a6 = 0,$$



$$b1 = 0,$$

$$b2 = 0,$$

$$b3 = x1,$$

$$b4 = x2,$$

$$b5 = 0,$$

$$b6 = -x3,$$

$$c1 = (-beta(i) * j) * x4,$$

$$c2 = (-beta(i) * j) * x4,$$

$$c3 = ((p/W) * y1) + ((p/U) * y2),$$

$$c4 = ((p/W) * y1) + ((p/U) * y3),$$

$$c5 = 0,$$

$$c6 = 0,$$

$$d1 = ((q * n2^2 * y1) / W) + ((q * n1^2 * y2) / U),$$

$$d2 = ((q * n2^2 * y1) / W) + ((q * n1^2 * y3) / U),$$

$$d3 = beta(i) * j * x4,$$

$$d4 = beta(i) * j * x4,$$

$$d5 = 0,$$

$$d6 = 0,$$

$$e1 = (beta(i) * j * x1) / (U^2 * C),$$

$$e2 = (beta(i) * j * x2) / (U^2 * C),$$

$$e3 = (-p * y6) / U,$$

$$e4 = (-p * y4) / U,$$

$$e5 = (\text{beta}(i) * j * x3) / (W^2 * C),$$

$$e6 = (-p * y5) / W,$$

$$f1 = (-q * n1^2 * y6) / U,$$

$$f2 = (-q * n1^2 * y4) / U,$$

$$f3 = (-\text{beta}(i) * j * x1) / (U^2 * C),$$

$$f4 = (-\text{beta}(i) * j * x2) / (U^2 * C),$$

$$f5 = (-q * n2^2 * y5) / W,$$

$$f6 = (-\text{beta}(i) * j * x3) / (W^2 * C),$$

**matr1 = [ a1 a2 a3 a4 a5 a6**

**b1 b2 b3 b4 b5 b6**

**c1 c2 c3 c4 c5 c6**

**d1 d2 d3 d4 d5 d6**

**e1 e2 e3 e4 e5 e6**

**f1 f2 f3 f4 f5 f6],**      **% places each element in the matrix**

**deter(i) = det(matr1),**      **% calculates the determinant of the matrix**

**m(i) = deter(i)/deter(i-1),**      **% divides determinany value of matrix by**

**% previous determinant value**

**if (m(i) < 0 0),**      **% if sign change has occurred**

```

if (deter(i-2)) ~= 0 0, % eliminates false roots

    U_t(j+1,x) = u(i) - ((deter(i) * delta) / (deter(i) - deter(i-1))),

    % calculates exact value of core mode parameter

    beta_t(x) = sqrt((n1^2*k^2) - (U_t(j+1,x)^2/in_rad^2)),

    % calculates value of corresponding propagation constant

    W_t(j+1,x) = in_rad* sqrt(beta_t(x)^2 - (n2^2*k^2)),

    % calculates value of corresponding cladding mode parameter

    fprintf(fid,'%0f %0f %f %f\n',j,x,U_t(j+1,x),W_t(j+1,x)),

    % prints l, m, U and W to the output file

    flag = 1, % i needs to be incremented by 10

    save djc mat, % saves all variables in the workspace

end, % end of true roots 'if' statement

end, % end of sign change 'if' statement

if flag == 1, % if a root has been found

    x = x + 1, % increment mode count

    t = 1, % reset delta step size to 1

    i = i + 10 % to separate stored determinant values in 'deter' array

    flag = 0, % reset flag

end, % end of positive flag 'if' statement

i = i + 1, % increment 'i' counter

ux = ucut(j+1,x) + (t*delta) + 0.01, % ux is a variable used for checking

if ux >= (U_max - 2*delta) % if the next cut-off value is greater than

```

U\_max

```

        i = limit,                % to break out of loop

        x = 0,                    % reset mode counter

        u = u*0,                  % reset u array

        deter = deter*0,          % reset deter array values

    end,                          % end of if loop

end,                              % end of 'while i < limit' loop

end,                              % end of 'for j = 0 j_lim' loop

fclose('all'),                   % closes all open files

```

## Appendix D

```
% Program title  holl_se m

% Purpose  To compute the coefficients appropriate to each allowed mode in a hollow cylindrical

% waveguide

% Method  A 5 * 5 determinant will be inverted and multiplied by a column matrix to extract the

% coefficients

% The 5*5 matrix consists of 5 lines taken from the 6*6 matrix in holl m, with all of the first column

% moved to a column matrix to form the constants


j = 1,                                % sets j back to 1 after exiting the previous program

p = - k * Z,                          % substitutional variable

q = k / Z,                            % substitutional variable

x = 1,                                % sets x back to 1 after exiting the previous program


beta(1) = n1*k,                       % sets first propagation constant value

fid2 = fopen('hollse dat','w'),        % opens a file for the output data

[limit,maxmode] = size(U_t),           % finds the size of the Matrix containing the true U

                                        % (core mode parameter) values


i = 1,

for j = 0 limit-1,                    % loops through all mode orders

    x = 1,                            % sets mode index (within each order) to 1
```

```

while x <= maxmode,

    coe = coe * 0;                                % matrix to hold coefficient values set to zero.

    U = U_t(j+1,x);                                % U value is retrieved from the holding matrix.

    beta(i) = sqrt((n1^2*k^2) - (U^2/in_rad^2));    % calculates the propagation constant.

    W = W_t(j+1,x);                                % W value is retrieved from the holding matrix.

    UC = out_rad * sqrt((n1^2*k^2) - beta(i)^2);    % calculates U*C.

    WC = out_rad * sqrt(beta(i)^2 - (n2^2*k^2));    % calculates W*C.


    BJU = besseli(j,U);                            % calculates value of bessel J at U.

    DBJU = -besseli(j+1,U) + (j/U)*BJU;            % calculates derivative of bessel J at U.


    BJUC = besseli(j,UC);                          % calculates value of bessel J at UC.

    DBJUC = -besseli(j+1,UC) + (j/UC)*BJUC; % calculates derivative of bessel J at UC.


    BYU = besseli(j,U);                            % calculates value of bessel Y at U.

    DBYU = -besseli(j+1,U) + (j/U)*BYU;            % calculates derivative of bessel Y at U.


    BYUC = besseli(j,UC);                          % calculates value of bessel Y at UC.

    DBYUC = -besseli(j+1,UC) + (j/UC)*BYUC; % calculates derivative of bessel Y at UC.


    BIW = besseli(j,W);                            % calculates value of bessel I at W.

    DBIW = besseli(j+1,W) + (j/W)*BIW ;           % calculates derivative of bessel I at W.

```

```

BKWC = besserk(j,WC), % calculates value of besserk K at WC

DBKWC = -besserk(j+1,WC) + (j/WC)*BKWC, % calculates derivative of besserk K at WC


BKW = besserk(j,W), % calculates value of besserk K at W

DBKW = -besserk(j+1,W) + (j/W) * BKW, % calculates derivative of besserk K at W


% x1-4 and y1-6 are substitutional variables used in the matrix

x1 = BJUC / BJU,

x2 = BYUC / BYU,

x3 = BKWC / BKW,

x4 = (1/U^2) + (1/W^2),


y1 = DBIW / BIW,

y2 = DBJU / BJU,

y3 = DBYU / BYU,

y4 = DBYUC / BYU,

y5 = DBKWC / BKW,

y6 = DBJUC / BJU,


%*****

if j == 0, % for zero order modes only separate
method is

temp1 = ((n2^2 * y1)/W) + ((n1^2 * y2)/U), % used to calculate coefficients

```

```

temp2 = ((n2^2 * y1)/W) + ((n1^2 * y3)/U),

coe(1) = (-temp1)/(temp2), % first coefficient is found

coe(4) = (x1 + (x2 * coe(1))) / x3, % fourth coefficient is found

coe(2) = 0, % all others are set to zero

coe(3) = 0,

coe(5) = 0,

else % if mode order is not zero

% the following are the elements of the 5*5 matrix,

a2 = x2,

a3 = 0,

a4 = 0,

a5 = -x3,

a6 = 0,

c2 = (-beta(i) * j) * x4,

c3 = ((p/W) * y1) + ((p/U) * y2),

c4 = ((p/W) * y1) + ((p/U) * y3),

c5 = 0,

c6 = 0,

d2 = ((q * n2^2 * y1) / W) + ((q * n1^2 * y3) / U),

d3 = beta(i) * j * x4,

d4 = beta(i) * j * x4,

```



$$d5 = 0,$$

$$d6 = 0,$$

$$e2 = (\text{beta}(i) * j * x2) / (U^2 * C),$$

$$e3 = (-p * y6) / U,$$

$$e4 = (-p * y4) / U,$$

$$e5 = (\text{beta}(i) * j * x3) / (W^2 * C),$$

$$e6 = (-p * y5) / W,$$

$$f2 = (-q * n1^2 * y4) / U,$$

$$f3 = (-\text{beta}(i) * j * x1) / (U^2 * C),$$

$$f4 = (-\text{beta}(i) * j * x2) / (U^2 * C),$$

$$f5 = (-q * n2^2 * y5) / W,$$

$$f6 = (-\text{beta}(i) * j * x3) / (W^2 * C),$$

matr1 = [ a2 a3 a4 a5 a6                   % puts each element of the 5\*5 matrix in the correct

          c2 c3 c4 c5 c6                   % position

          d2 d3 d4 d5 d6

          e2 e3 e4 e5 e6

          f2 f3 f4 f5 f6 ],

% the following are the elements of the column matrix

$$a1 = -x1,$$

$$c1 = (\text{beta}(i) * j) * x4,$$

```

d1 = ((-q * n2^2 * y1) / W) - ((q * n1^2 * y2) / U),

e1 = (-beta(i) * j * x1) / (U^2 * C),

f1 = (q * n1^2 * y6) / U,


matr2 = [a1, c1, d1, e1, f1],      % sets up the column matrix

coe = matr1 \ matr2,      % multiplies inverse of matr1 by column matrix

end,      % the '\' is a special matlab character for this operation

fprintf(fid2, '\n% 0f % 0f % 4f % 4f', j, x, U_t(j+1, x), W_t(j+1, x)),

fprintf(fid2, ' % 5f % 5f % 5f % 5f % 5f\n', coe(1), coe(2), coe(3), coe(4), coe(5)),

% the order, mode index m, U value, W value and the corresponding coefficients are output to a file


if x < maxmode,      % if the last mode in a given order has not been reached

    if U_t(j+1, x+1) == 0,      % if the next mode of that order is zero

        x = maxmode + 1,      % make x > maxmode

    end,

end,      % end of 'x < maxmode' loop

x = x+1,      % increment x

end,      % end of 'while x <= maxmode' loop

end,      % end of 'for j = 0 limit-1' loop

fclose('all'),      % close all open files

save c \hollse mat      % save variable values in a matlab workspace file

```

## Appendix E

```
% Title  hollpow m

% Object  To calculate the power ratio in a hollow cylindrical waveguide

% Method  To numerically integrate over all allowed modes in annulus


j = 1,                % set mode order no back to 1

p = - k * Z,          % substitututonal variable

q = k / Z,            % substitututonal variable

x = 1,                % set mode order index to 1

beta(1) = n1*k,        % set first value of propagation constant


AA = 1,                % AA is first coefficient, and was set to 1 in previous program to enable
the

                        % calculation of the other coefficients

fid = fopen('hollse dat','r'),    % opens the file to which Hollse m saved the results of its run

in_data = fscanf(fid,'%f\n'),      % reads in the data as one column

fclose(fid),                      % closes the file

limit = length(in_data),          % calculates the number of variables in the column of data


i = 1,                            % set index equal to 1, the first element of the data column

while i <= limit,                  % read in nine values for each single mode

    j = in_data(i),                % each input value is assigned a label and stored
```

```

x = in_data(i+1),

U_t(j+1,x) = in_data(i+2),

W_t(j+1,x) = in_data(i+3),

BB(j+1,x) = in_data(i+4),

CC(j+1,x) = in_data(i+5),

DD(j+1,x) = in_data(i+6),

EE(j+1,x) = in_data(i+7),

FF(j+1,x) = in_data(i+8),

i = i+9,          % index incremented by nine to the next set of nine values

end,              % end of data storage loop

j_limit = in_data(i-9),      % sets the maximum value of j

[qwe,x_limit] = size(U_t),    % finds the size of the array holding the U values

U_t(j_limit,x_limit+1) = 0,   % increases the array columns by 1, and sets that column = 0

fid1 = fopen('hollpow5 dat','w'), % opens a file for output data


F1 = 0,           % the variables that will store the power fractions are set to 0

F2 = 0,

F3 = 0,

mode_count = 0,   % the mode counter is set to 0

for j = 0:j_limit,      % loop through all the mode orders

    x = 0,             % sets mode index to 0

    while x < x_limit,  % while mode index is less than its maximum value

        x = x + 1,      % increment mode index

```

$U = U_t(j+1, x)$ , % retrieve corresponding U value

$W = W_t(j+1, x)$ , % retrieve corresponding W value

$\beta = \sqrt{(n_1^2 k^2 - (U^2 / \ln_{\text{rad}}^2))}$ , % calculate corresponding prop const

$BJU = \text{besselj}(j, U)$ , % calculates bessel J at U

$DBJU = -\text{besselj}(j+1, U) + (j/U) * BJU$ , % calculates derivative of bessel J at U

$BYU = \text{bessely}(j, U)$ , % calculates bessel Y at U

$DBYU = -\text{bessely}(j+1, U) + (j/U) * BYU$ , % calculates derivative of bessel Y at U

$BIW = \text{besseli}(j, W)$ , % calculates bessel I at W

$DBIW = \text{besseli}(j+1, W) + (j/W) * BIW$ , % calculates derivative of bessel I at W

$BKW = \text{besselk}(j, W)$ , % calculates bessel K at W

$DBKW = -\text{bessel}(j+1, W) + (j/W) * BKW$ , % calculates derivative of bessel K at W

% the following are substitutional variables

$a1 = (\beta * (AA + BB(j+1, x))) / (W * BIW)$ ,

$a2 = (p * j * (CC(j+1, x) + DD(j+1, x))) / (W^2 * BIW)$ ,

$a3 = (\beta * j * (CC(j+1, x) + DD(j+1, x))) / (W^2 * BIW)$ ,

$a4 = (q * n_2^2 * (AA + BB(j+1, x))) / (W * BIW)$ ,

$b1 = (-\beta * AA) / (U * BJU)$ ,

$$b2 = (-\text{beta} * BB(j+1,x)) / (U * BYU),$$

$$b3 = (-p * j * CC(j+1,x)) / (U^2 * BJU),$$

$$b4 = (-p * j * DD(j+1,x)) / (U^2 * BYU),$$

$$b5 = (-\text{beta} * j * CC(j+1,x)) / (U^2 * BJU),$$

$$b6 = (-\text{beta} * j * DD(j+1,x)) / (U^2 * BYU),$$

$$b7 = (-q * n1^2 * AA) / (U * BJU),$$

$$b8 = (-q * n1^2 * BB(j+1,x)) / (U * BYU),$$

$$c1 = (\text{beta} * EE(j+1,x)) / (W * BKW),$$

$$c2 = (p * j * FF(j+1,x)) / (W^2 * BKW),$$

$$d1 = (\text{beta} * j * FF(j+1,x)) / (W^2 * BKW),$$

$$d2 = (q * n2^2 * EE(j+1,x)) / (W * BKW),$$

$$e1 = (-\text{beta} * j * (AA+BB(j+1,x))) / (W^2 * BIW),$$

$$e2 = (p * (CC(j+1,x)+DD(j+1,x))) / (W * BIW),$$

$$f1 = (\text{beta} * (CC(j+1,x)+DD(j+1,x))) / (W * BIW),$$

$$f2 = (-n2^2 * q * j * (AA+BB(j+1,x))) / (W^2 * BIW),$$

$$g1 = (\text{beta} * j * AA) / (U^2 * BJU),$$

$$g2 = (\text{beta} * j * BB(j+1,x)) / (U^2 * BYU),$$

$$g3 = (-p * CC(j+1,x)) / (U * BJU),$$

$$g4 = (-p * DD(j+1,x)) / (U * BYU),$$

$$h1 = (-beta * CC(j+1,x)) / (U * BJU),$$

$$h2 = (-beta * DD(j+1,x)) / (U * BYU),$$

$$h3 = (n1^2 * q * AA) / (U^2 * BJU),$$

$$h4 = (n1^2 * q * BB(j+1,x)) / (U^2 * BYU),$$

$$i1 = (-beta * j * EE(j+1,x)) / (W^2 * BKW),$$

$$i2 = (p * FF(j+1,x)) / (W * BKW),$$

$$j1 = (beta * FF(j+1,x)) / (W * BKW),$$

$$j2 = (-n2^2 * q * j * EE(j+1,x)) / (W^2 * BKW),$$

%\*\*\*\*\*

R\_min1 = 0 0,                   % sets the smallest radius of the waveguide

R\_min2 = 1,                   % radius at inner interface of cladding and core

R\_min3 = C,                   % radius at inner interface of cladding and core

R\_min4 = 2\*C,               % radius at outer surface of cladding

deltaR = 0 01,               % step size used to increment radius

maxN1 = R\_min2 / deltaR,       % number of steps from R = 0 to R = 1

maxN2 = ((R\_min3 - R\_min2)\*2) / deltaR, % number of steps from R = 1 to R = C

maxN3 = (R\_min4 - R\_min3) / deltaR,   % number of steps from R = C to 2\*C

```

sum1 = 0,

for N = 1 maxN1,                                % from R = 0 to R = 1

    R = R_min1 + (N * deltaR),                    % calculate radius

    UR = R * in_rad * sqrt((n1^2*k^2) - beta^2),    % U*R

    WR = R * in_rad * sqrt(beta^2 - (n2^2*k^2)),    % W*R

    BIWR = besseli(j,WR),                        % bessel I at W*R

    DBIWR = besseli(j+1,WR) + (j/WR)*BIWR ,        % derivative of bessel

                                                    % I at W*R

    term1 = (a1 * DBIWR) + ((a2 * BIWR)/R), % substitutional variables

    term2 = ((a3 * BIWR)/R) + (a4 * DBIWR),

    term3 = ((e1 * BIWR)/R) + (e2 * DBIWR),

    term4 = (f1 * DBIWR) + ((f2 * BIWR)/R),

    total(1) = (term1 * term2) - (term3 * term4),

    total(1) = abs(total(1)), % calculates power at each radius

    sum1 = sum1 + (total(1) * R * deltaR), % running total of power values

end,                                              % end of inner section loop

sum2 = 0,

for N = 1 maxN2                                % from R = 1 to R = C

    R = R_min2 + (N * deltaR),                    % calculates radius

```



```

UR = R * m_rad * sqrt((n1^2*k^2) - beta^2),      % U*R

WR = R * m_rad * sqrt(beta^2 - (n2^2*k^2)),      % W*R


BJUR = besselj(j,UR),                          % bessell J at UR

DBJUR = -besselj(j+1,UR) + (j/UR)*BJUR, % derivative of bessell J at UR


BYUR = bessely(j,UR),                          % bessell Y at UR

DBYUR = -bessely(j+1,UR) + (j/UR)*BYUR,          % derivative of bessell
                                                    % Y at UR


% substitutional variables


term1 = (b1 * DBJUR) + (b2 * DBYUR) + ((b3 * BJUR)/R) + ((b4 *
BYUR)/R),

term2 = ((b5 * BJUR)/R) + ((b6 * BYUR)/R) + (b7 * DBJUR) + (b8 *
DBYUR),

term3 = ((g1 * BJUR)/R) + ((g2 * BYUR)/R) + (g3 * DBJUR) + (g4 *
DBYUR),

term4 = (h1 * DBJUR) + (h2 * DBYUR) + ((h3 * BJUR)/R) + ((h4 *
BYUR)/R),

total(2) = (term1 * term2) - (term3 * term4),

total(2) = abs(total(2)),    % calculates power at each radius


sum2 = sum2 + (total(2) * R * deltaR), % running total of power values

end,    % end of glass annulus loop

```

```

sum3 = 0,

for N = 1 maxN3,                                % from R = C to 2*C

    R = R_min3 + (N * deltaR),                    % calculates radius

    UR = R * in_rad * sqrt((n1^2*k^2) - beta^2),    % U*R

    WR = R * in_rad * sqrt(beta^2 - (n2^2*k^2)),    % W*R

    BKWR = besserk(j,WR),                        % bessell K of WR

    DBKWR = -besserk(j+1,WR) + (j/WR)*BKWR,        % derivative of bessell

                                                % K of WR

% substitutional variables

term1 = (c1 * DBKWR) + ((c2 * BKWR)/R),

term2 = ((d1 * BKWR)/R) + (d2 * DBKWR),

term3 = ((i1 * BKWR)/R) + (i2 * DBKWR),

term4 = (j1 * DBKWR) + ((j2 * BKWR)/R),

total(3) = (term1 * term2) - (term3 * term4),

total(3) = abs(total(3)),    % calculates power at each radius

sum3 = sum3 + (total(3) * R * deltaR), % running total of power values

end,                                % end of outer cladding loop

% power fractions for each section of the waveguide are calculated

R1 = sum1/(sum1 + sum2 + sum3),

R2 = sum3/(sum1 + sum2 + sum3),

R3 = sum2/(sum1 + sum2 + sum3),

```

```

        fprintf(fid1,'% 0f    % 0f    % 4f    % 4f    % 4e    % 4e    % 4e    % 4e\n',
j,x,U,W,R1,R2,R3,R1+R2),                % outputs mode parameters and power fractions

F1 = F1 + R1,                            % running totals of power fractions

F2 = F2 + R2,

F3 = F3 + R3,

mode_count = mode_count + 1,    % mode count is incremented

if U_t(j+1,x+1) == 0,                % if last mode for this order has been reached

    x = x_limit,                    % break out of mode index loop, move to next

    % mode

end,

end,                                    %end of x loop

end,                                    %end of j loop

fclose(fid1),                        % close output file

F1 = F1/mode_count                    % output average power fractions to screen

F2 = F2/mode_count

F3 = F3/mode_count

```

# Appendix F

This program controls the running of all the other programs needed to calculate power fractions for the hollow cylindrical waveguide probe. Variables named in this program become common to all the programs called by this one.

% Title Modes m

% Aim To combine all steps to calculate power fractions in a hollow cylindrical waveguide

% The following are commands to obtain information from the program user

n1 = input('Enter the refractive index of the glass '),

n2 = input('Enter the refractive index of the cladding '),

lambda = input('What is the excitation wavelength ? '),

in\_rad = input('What is the inner radius dimension ? '),

out\_rad = input('What is the outer radius dimension ? '),

% the following are examples of values that could be used by the program

%n1 = 1.46

%n2 = 1.45

%lambda = 1e-6

%in\_rad = 80e-6

%out\_rad = 100e-6

C = out\_rad/in\_rad, % ratio of inner radius to outer radius

```

k = (2 * pi)/ lambda,          % defines the wavenumber, k

Z = 377,                        % the characteristis impedance of free space

x_max = (in_rad * sqrt((n1^2*k^2) - n2^2 * k^2)) + 30,    % max x value used in finding cut-off
                                                    % values

j_max = x_max + 35,            % max j value used in finding cut-off values

cuts,                          % each program is called in order of use

holl,

holl_se,

hollpow,

```

## Appendix G

In the text of Chapter 4, section 2.6, it was assumed that all modes in the hollow waveguide were reflected with the same reflection coefficient  $R$  at the end face (silica-silver interface). This is proved in this appendix for the range of incident angles within which the quasi plane waves strike the glass-silver interface.

For reflection at an interface (for light whose  $E$  field is in the plane of incidence) the reflected  $E$  field amplitude  $E_r$  is related to the incident value by the expression (due to Fresnel)

$$\frac{E_r}{E_i} = \frac{Z_2 \cos \theta_2 - Z_1 \cos \theta_1}{Z_2 \cos \theta_2 + Z_1 \cos \theta_1} \quad \text{Eqn G-1}$$

(see Pain, (1968))

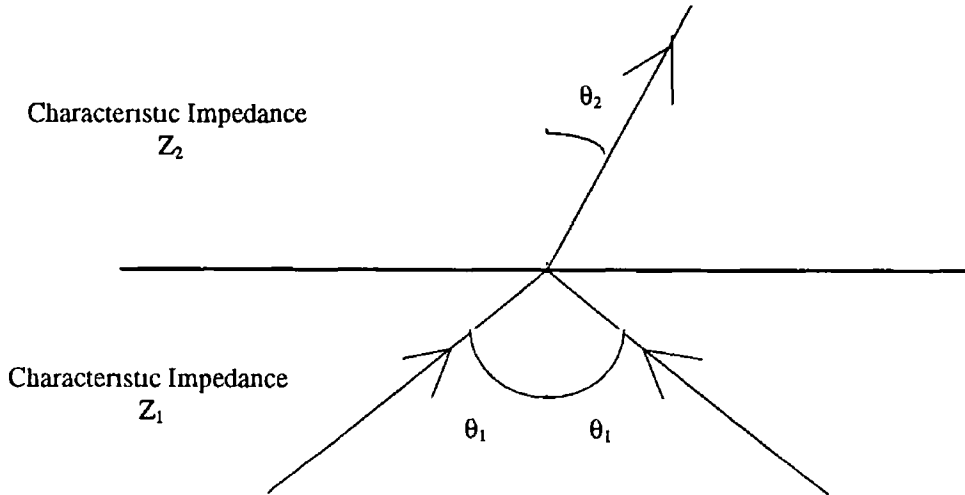


Figure G-1 Reflection and transmission at an interface between two media.

Now  $Z_2 = Z_0 / n_2$  and  $Z_1 = Z_0 / n_1$  ( $Z_0 = 377 \Omega$  = characteristic impedance of free-space (or vacuum))

For silica ( $n_1 = 1.46$ ) surrounded by a methanol solution ( $n_2 = 1.329$ ) the critical angle is  $65.5^\circ$ . For a launch numerical aperture of 0.37 we can write

$$0.37 = 1.46 \sin \theta_{\text{incident}} = 1.329 \sin \theta_{\text{max}} \quad \text{Eqn G-2}$$

$$\text{i.e. } \theta_{\text{max}} = 68^\circ$$

$\theta_{\max}$  is the maximum value of the incident angle within the waveguide

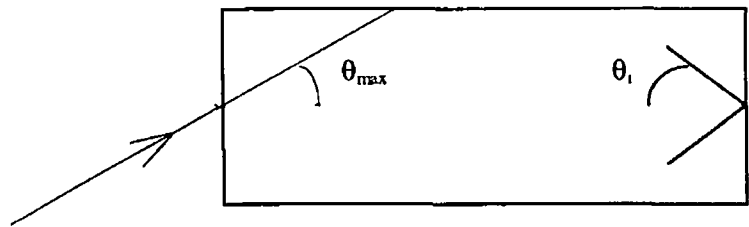


Figure G-2 Light ray undergoing total internal reflection

Because of total internal reflection, the maximum value of  $\theta_1$  at the distal end is by symmetry also  $14.68^\circ$ . By Snell's Law the transmitted angle  $\theta_2$  (maximum) is given by

$$1.46 \sin 14.68^\circ = 1.329 \sin (\theta_2)$$

$$\text{i.e. } \theta_{2(\text{maximum})} = 16.165^\circ$$

Using equation G-1, R is then

$$\frac{(1.46)[\cos(16.16)] - 1.329[\cos(14.68)]}{(1.46)[\cos(16.16)] + 1.329[\cos(14.68)]} = 0.0434 \quad \text{Eqn G-3}$$

At normal incidence  $\theta_1 = \theta_2 = 0$ , the amplitude reflection coefficient is

$$\frac{1.46 - 1.329}{1.46 + 1.329} = 0.0487 \quad \text{Eqn G-4}$$

or about 12% larger than the minimum possible value (which occurs at  $\theta_{1(\max)}$  of  $16.16^\circ$ ) shown in equation G-3 above. Over the full range of possible mode incident angles, then it is not unreasonable to assume a constant reflection coefficient R for all modes as adopted in equation 4.5.2

## ***Appendix F References.***

**Pain HJ**            “The Physics of Vibrations and Waves” (Wiley & Sons NY, 1968) Chapter 7, p208



$\frac{J_i(UC)}{J_i(U)}$	$\frac{Y_i(UC)}{Y_i(U)}$	0
0	0	$\frac{J_i(UC)}{J_i(U)}$
$-\beta l \left( \frac{1}{U^2} + \frac{1}{W^2} \right)$	$-\beta l \left( \frac{1}{U^2} + \frac{1}{W^2} \right)$	$\frac{p}{W} \frac{I'_i(W)}{I_i(W)} + \frac{p}{U} \frac{J'_i(U)}{J_i(U)}$
$\frac{qn_2^2}{W} \frac{I'_i(W)}{I_i(W)} + \frac{qn_1^2}{U} \frac{J'_i(U)}{J_i(U)}$	$\frac{qn_2^2}{W} \frac{I'_i(W)}{I_i(W)} + \frac{qn_1^2}{U} \frac{Y'_i(U)}{Y_i(U)}$	$\beta l \left( \frac{1}{U^2} + \frac{1}{W^2} \right)$
$\frac{\beta l}{U^2 C} \frac{J_i(UC)}{J_i(U)}$	$\frac{\beta l}{U^2 C} \frac{Y_i(UC)}{Y_i(U)}$	$-\frac{p}{U} \frac{J'_i(UC)}{J_i(U)}$
$-\frac{qn_1^2}{U} \frac{J'_i(UC)}{J_i(U)}$	$-\frac{qn_1^2}{U} \frac{Y'_i(UC)}{Y_i(U)}$	$-\frac{\beta l}{U^2 C} \frac{J_i(UC)}{J_i(U)}$

# Appendix H

0	$-\frac{K_l(WC)}{K_l(W)}$	0
$\frac{Y_l(UC)}{Y_l(U)}$	0	$-\frac{K_l(WC)}{K_l(W)}$
$\frac{p}{W} \frac{I_l'(W)}{I_l(W)} + \frac{p}{U} \frac{Y_l'(U)}{Y_l(U)}$	0	0
$\beta l \left( \frac{1}{U^2} + \frac{1}{W^2} \right)$	0	0
$-\frac{p}{U} \frac{Y_l'(UC)}{Y_l(U)}$	$\frac{\beta l}{W^2 C} \frac{K_l(WC)}{K_l(W)}$	$-\frac{p}{W} \frac{K_l'(WC)}{K_l(W)}$
$-\frac{\beta l}{U^2 C} \frac{Y_l'(UC)}{Y_l(U)}$	$-\frac{qn_2^2}{W} \frac{K_l'(WC)}{K_l(W)}$	$-\frac{\beta l}{W^2 C} \frac{K_l(WC)}{K_l(W)}$